A SINGLE CRYSTAL SODIUM IODIDE SCINTILLATION SPECTROMETER FOR THE INVESTIGATION OF GAMMA-RAY SPECTRA

by

Richard Ernest Azuma

A THESIS SUBMITTED IN PARTIAL FULFILMENT OF THE REQUIREMENTS FOR THE DEGREE OF

MASTER OF ARTS

in the Department

of

PHYSICS

We accept this thesis as conforming to the standard required from candidates for the degree of MASTER OF ARTS

Members of the Department of

PHYSICS

THE UNIVERSITY OF BRITISH COLUMBIA
April, 1953

ABSTRACT

A single crystal sodium iodide spectrometer has been developed for the investigation of gamma-ray spectra. The spectrometer was tested with the gamma-rays from the sources Eu^{155}, RaD, Na^{22}, Zn^{65}, Co^{60}, and RdTh. The spectra from these sources have been obtained by analyzing the pulse height distribution from the scintillation counter with a single channel differential discriminator.

A crystal mounting technique is described in which the crystals are mounted dry with a layer of magnesium oxide powder surrounding them to provide diffuse reflecting surfaces. With mountings of this type, 7% energy resolution has been achieved for gamma-ray energies of approximately 1 MeV.

The expected pulse height distributions have been calculated and compared with the experimental distributions. The effect of multiple scattering events on the shape of the distributions is discussed, and the effect of crystal dimensions on the resolution has been studied. It has been found that for the energy region 0.5 to 2.5 MeV the best resolution is obtained with small crystals.

A search has been made for the presence of low energy gamma-rays in the decay of tritium, and it was found that within the accuracy of the experiment no gamma-rays were present.

A preliminary report is presented on the investigation of possible scintillation produced in air by alpha particles. The effect has been shown to exist but no systematic study has been made.

ACKNOWLEDGMENTS

The author wishes to express his thanks to Dr. J. B. Warren for suggesting this research and for his advice and supervision in performing the experiments.

Thanks are also due to Mr. G. M. Griffiths for his many helpful discussions and suggestions.

The author also wishes to thank the National Research Council for the Summer Research Grant and Bursary under which this research was carried out.

INDEX

ILLUSTRATIONS

Figure Number — Facing Page

TABLES

Number

PLATES

Number

I. INTRODUCTION

The development of the scintillation counter as an energy sensitive detector has produced a powerful tool for the study of X-ray and gamma-ray spectra. Recent refinements in technique have resulted in the design of spectrometers which are capable of measuring gamma-ray spectra from sources of the order of 10^{-9} curie and with resolution, (measured as the ratio of the full width at half maximum to energy at peak), of approximately 8 percent, for the energy region 1 to 3 MeV. This definition of energy resolution will be used throughout the text. The resolution attainable, to date, for the energy region below 1 MeV has been restricted by the statistical variations associated with the photomultiplier tubes, and below 100 KeV, these variations become dominant and a resolution of about 40% can be expected, getting worse as the energy drops. The poor resolution in this very low energy region may quite often be tolerated since the high efficiency of the scintillation counter makes possible the detection and measurement of spectra from extremely weak sources.

The use of thallium-activated sodium iodide crystals as a means of distinguishing gamma-ray energies was first reported by R. Hofstadter in 1948 (1). This initial report showed that the fluorescent light output of sodium iodide was considerably larger than that from most of the known organic phosphors, but not anthracene, and that the intensity of fluorescence was an increasing function of the incident gamma-ray energy. A subsequent publication by the same author (2) showed that sodium iodide counters gave a characteristic pulse height distribution for an incident

beam of monoenergetic gamma-rays. This "spectrum" was characterized by the presence of a continuous distribution with a sharp cut-off at the high energy side, and by the presence of a number of sharp peaks. The peaks were attributed to the interaction of the gamma-rays with the heavy component (iodine, z=53) of the crystal by means of the photoelectric and pair production processes, and the continuous distribution was interpreted as the result of interactions by the Compton effect. The position of the photoelectric and pair peaks in the distribution was reported to be a linear function of the incident gamma-ray energy. This linearity with respect to incident gamma-ray energy of the fluorescent output of the crystal, along with the presence of sharp peaks in the spectrum, and the high absorption efficiency has made sodium iodide the ideal type of crystal to use for the measurement of gamma-ray energies.

Recent advances in the design of photomultiplier tubes have resulted in marked improvement in the performance of the scintillation counter. Those factors of photomultiplier design which are of most importance in this application are the following:

(i) High efficiency in photocathode emission, and uniformity of emission over the whole photocathode surface.

(ii) High gain and low dark current.

(iii) Large photocathode area to increase light collection efficiency.

(iv) Insensivitity of the gain to stray magnetic fields.

(v) Large output current pulse without affecting linearity of the response or causing ion feedback.

(vi) Maximum efficiency in collection of the electrons from the photocathode.

(vii) Matching of the spectral response of the photocathode with that of the fluorescent radiation of the crystal.

Although much research has been done to improve these operating characteristics, the statistical fluctuations introduced by them, especially variations in photocathode emission and gain, still account for approximately half of the observed spread of the peaks.

The spurious pulses produced by thermionic emission from the dynodes of the photomultiplier are of the same magnitude as those pulses produced by very low energy gamma-rays and X-rays. These spurious pulses may be reduced both in magnitude and in number by cooling the tube to liquid air temperatures. Hence the spectra of very weak intensity, low energy gamma-rays, (< 1 KeV) may be investigated but this method has not as yet been exploited to its fullest extent.

The effect of the uniformity of the crystal (i.e. uniform fluorescent yield from all parts of the crystal for a given gamma-ray energy), the size of the crystal, the method of mounting the crystal, and the degree of collimation of the incident gamma-ray beam on the energy resolution of the counter has been described in the literature (2,3,4). Invesitgation has shown that aside from improved photomultiplier tubes and uniformity in crystals, the largest single gain in resolution is obtained by improved crystal mounting techniques. R.K. Swank has outlined (5) a method of mounting sodium iodide crystals in order to ob-

tain optimum light input into the multiplier and hence optimum resolution. With this method as a guide, a crystal mounting technique has been developed which is capable of producing a counter with a resolution, for example, of seven percent for the two photoelectric lines in the spectrum of Co^{60}.

The techniques of scintillation spectrometry as introduced above has been used in the performance of many kinds of experiments. A few of the more well known types of experiments are listed below:

(i) The detection and measurement of gamma-ray spectra (especially in the case of weak intensity spectra) produced by bombardment of target materials with accelerated particles.

(ii) The search for weak intensity gamma-rays from isotopes.

(iii) The determination of cross-sections in "bombardment" experiments, and absolute flux measurement of line gamma-rays.

(iv) The determination of decay schemes by means of α-γ, β-γ and γ-γ coincidences.

(v) The measurements of internal conversion ratios by measuring the ratios of X-ray flux.

There are very many more specialized applications of this technique to particular experiments. So far this technique has been applied by the author only to (ii) mentioned above.

II. THE INTERACTION OF GAMMA-RAYS WITH THE CRYSTAL AND THE SPECTRUM SHAPE.

It has been shown (3,4) that the pulse height distribution obtained with a scintillation counter for an incident beam of mono-energetic gamma-rays has a characteristic shape. In order that the energy of the incident gamma-rays may be determined from this distribution an analysis must be made of the effect on the shape of the spectrum of each of the three absorption processes:

(i) Compton effect.

(ii) Photoelectric effect.

(iii) Pair production.

The crystal obtains its fluorescent energy from the energetic electrons which result from the absorption processes. The pulse distribution, in its general aspects, is then determined by the energy vs. number distribution of these electrons. These distributions are calculated below for each of the absorption processes, from which the "ideal" distribution can be calculated.

The "ideal" distribution is, of course, distorted due to multiple scattering events taking place in the crystal, wall effects, and by statistical fluctuations introduced by the photomultiplier tube. These effects are discussed below and a qualitative argument is presented of these effects on the shape of the distribution.

A. COMPTON EFFECT

In considering the Compton effect it is assumed that the electrons in the atom may be thought of as free and that the photon collides with an electron and is deflected, the electron recoiling

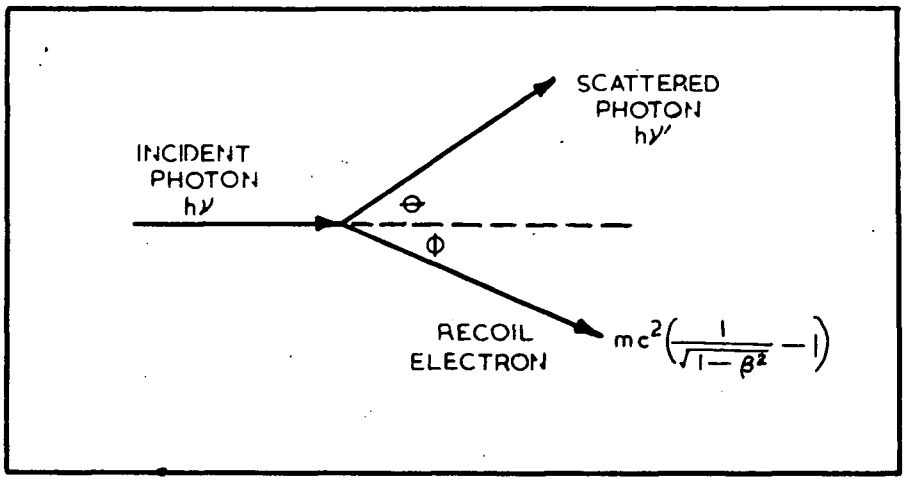

FIGURE I

The Compton Effect, Showing Angular and Energy Notations

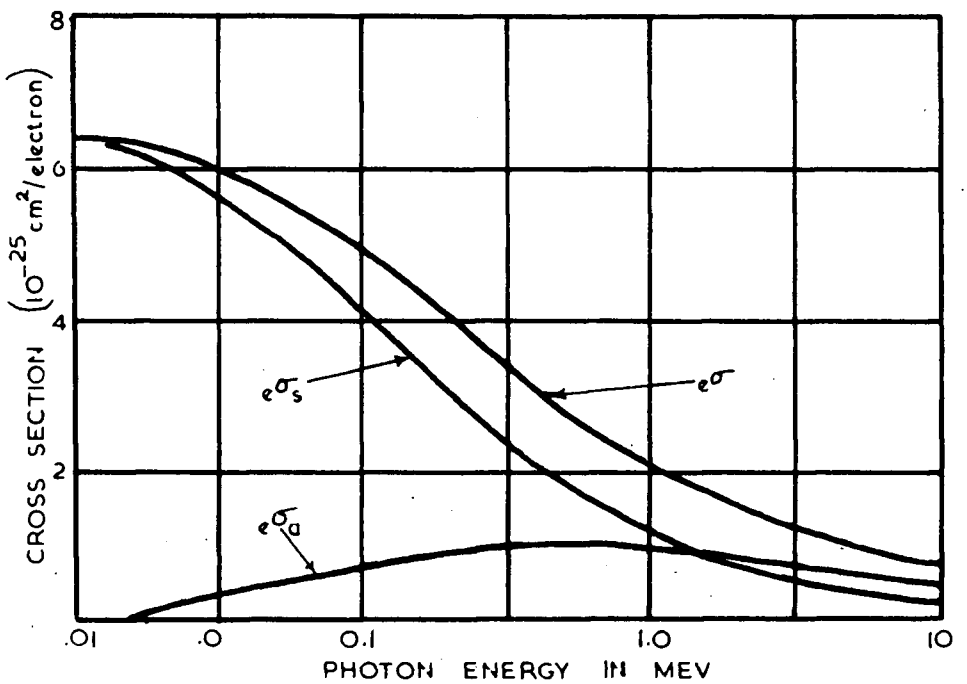

FIGURE II

Cross-Sections vs. Energy for the Compton Effect $e\sigma$ the cross-section for the number of photons scattered; $e\sigma_s$ the cross-section for the energy of the scattered photons; $e\sigma_a$ the cross-section for the energy absorbed by the electrons

in a different direction. It is the number vs. energy distribution of the recoil electrons that must be calculated. In the calculations that follow, it is assumed that only primary processes occur, i.e., all degraded quanta escape from the crystal with no further interactions, and that the electrons lose all their energy to the crystal (i.e., no wall effect) and radiate none in the form of brehmstrahlung radiation.

From the conservation of energy and momentum in the process, the relativistic equations for energy and mass, and the notation shown in Fig. (I), the following expressions can be obtained:

$$h\nu' = \frac{h\nu}{1+\alpha(1-\cos\theta)} \tag{1}$$

$$E_{el} = h\nu\left\{1-\frac{1}{1+\alpha(1-\cos\theta)}\right\} \tag{2}$$

$$= h\nu\left\{\frac{2\alpha}{1+2\alpha+(1+\alpha^2)\tan^2\phi}\right\} \tag{3}$$

$$\cos\theta = 1-\frac{2}{(1+\alpha)^2\tan^2\phi+1} \tag{4}$$

where $\alpha = \frac{h\nu}{mc^2}$

Klein and Nishina (6) have carried out a quantum mechanical calculation of the process and have obtained the following equation for the fraction of the gamma-ray energy scattered in a given direction:

$$I = I_o \frac{e^4}{2m^2c^4r^2} \frac{1+\cos^2\theta}{[1+\alpha(1-\cos\theta)]^3}\left\{1+\frac{\alpha^2(1-\cos\theta)}{(1+\cos^2\theta)[1+\alpha(1-\cos\theta)]}\right\} \tag{5}$$

where Io = intensity of incident beam of gamma-rays,

I = intensity of scattered beam at the angle θ and distance r from the scattering electron of charge e and mass m.

If $k(\theta)$ = cross-section for the number of photons scattered per electron and per unit solid angle in the direction θ, then equation (5) may be written $I = \frac{I_0}{r^2} \frac{h\nu'}{h\nu} k(\theta)$

where $k(\theta) = \frac{d_e\sigma(\theta)}{d\Omega} = \frac{r_0^2}{2}\left\{\frac{1}{[1+\alpha(1-\cos\theta)]^2}\left[1+\cos^2\theta+\frac{\alpha^2(1-\cos\theta)^2}{[1+\alpha(1-\cos\theta)]}\right]\right\}$ (6)

In the above equation

$$r_0^2 = \left(\frac{e^2}{mc^2}\right)^2 = cm^2$$

$_e\sigma(\theta)$ = cross-section for the number of photons scattered in to the solid angle $d\Omega$ in the direction θ. The cross-section for the amount of energy scattered per electron and per unit solid angle in the direction θ is

$$K(\theta) = \frac{h\nu'}{h\nu} k(\theta)$$

Combining equations (1) and (6) $K(\theta)$ becomes

$$K(\theta) = \frac{d_e\sigma_s(\theta)}{d\Omega} = \frac{r_0^2}{2}\left\{\frac{1}{[1+\alpha(1-\cos\theta)]^3}\left[1+\cos^2\theta+\frac{\alpha^2(1-\cos\theta)^2}{[1+\alpha(1-\cos\theta)]}\right]\right\} \quad (7)$$

where $_e\sigma_s(\theta)$ is the cross section for the energy of the photons scattered into solid angle $d\Omega$ in the direction θ.

If the following definitions are made:

(i) $_e\sigma$ = Compton total cross-section i.e., cross-section for the number of photons scattered or for the total amount of energy removed from the beam.

(ii) $_e\sigma_s$ = Compton scattering coefficient i.e., cross-section for the amount of energy retained by the scattered photons then $_e\sigma$ and $_e\sigma_s$ are obtained by integrating equations (6) and (7) respectively over all possible directions. The resulting equations are:

$$e\sigma = 2\pi r_o^2 \left\{ \frac{1+\alpha}{\alpha^2} \left[\frac{2(1+\alpha)}{1+2\alpha} - \frac{1}{\alpha} \ln(1+2\alpha) \right] + \frac{1}{2\alpha} \ln(1+2\alpha) - \frac{1+3\alpha}{(1+2\alpha)^2} \right\} \quad (8)$$

$$e\sigma_s = \pi r_o^2 \left[\frac{1}{\alpha^3} \ln(1+2\alpha) + \frac{2(1+\alpha)(2\alpha^2-2\alpha-1)}{\alpha^2(1+2\alpha)^2} + \frac{8\alpha^2}{3(1+2\alpha)^3} \right] \quad (9)$$

Since $e\sigma$ is the cross-section for the total amount of energy removed from the incident beam, and $e\sigma_s$ is the cross-section for the amount of energy retained by the scattered photons, then $e\sigma_a$ the cross-section for the amount of energy absorbed by the recoiling electrons is

$$e\sigma_a = e\sigma - e\sigma_s$$

C.M. Davisson (7) has calculated values for these cross-sections at various energies. They are shown in Fig. (II).

Since the probability that an electron will be scattered into $d\Omega'$ situated in the direction ϕ , is the same as the probability that a primary quantum will be scattered into the solid angle $d\Omega$ in the direction θ , θ and ϕ being related by equation (4), then

$$d_e\sigma(\phi) = k(\theta)\, d\Omega = k(\phi)\, d\Omega'$$

$$\frac{d_e\sigma(\phi)}{d\Omega'} = k(\phi) = k(\theta) \frac{d\Omega}{d\Omega'} \quad (10)$$

where $k(\theta)$ and $k(\phi)$ have analogous meaning, but are for photons and electrons respectively and where $k(\theta)$ is given by equation (6). Now, if equation (10) is integrated only over Φ (the polar angle Φ) the result obtained is

$$\frac{d_e\sigma'(\phi)}{d\phi} = 2\pi \sin\phi\, k(\theta) \frac{d\Omega}{d\Omega'} \quad (11)$$

where the prime on the σ indicates that the Φ dependence has been integrated out, and where $\frac{d_e\sigma'(\phi)}{d\phi}$ is the cross-section

for the number of electrons scattered between two cones whose half angles differ by unity.

The quantity of interest is the differential cross-section as a function of electron energy, which might be thought of as the number vs. energy distributions of the electrons. Mathematically this is

$$\frac{d_e\sigma'(\phi)}{dE_{el}} = \frac{d_e\sigma'(\phi)}{d\phi}\,\frac{d\phi}{dE_{el}} \tag{12}$$

$\frac{d\phi}{dE_{el}}$ can immediately be found by differentiating equation (3) and it is

$$\frac{d\phi}{dE_{el}} = -\frac{1}{4\alpha(1+\alpha)^2\,h\nu}\,\frac{\left[1+2\alpha+(1+\alpha)^2\tan^2\phi\right]^2}{\tan\phi\sec^2\phi} \tag{13}$$

In order to find $\frac{d_e\sigma'(\phi)}{d\phi}$ (see equation (11)), $\frac{d\Omega}{d\Omega'}$ must first be calculated.

If the polar coordinates are R, Θ and Φ, and if the scattering angle θ or ϕ is associated with the polar angle Θ, then the element of solid angle is

$$\text{for the photon } d\Omega = \sin\Theta\; d\theta\, d\Phi$$

$$\text{for the electron } d\Omega' = \sin\phi\; d\phi\, d\Phi$$

Thus $\frac{d\Omega}{d\Omega'} = \frac{\sin\theta\, d\theta}{\sin\phi\, d\phi}$

$\frac{d\theta}{d\phi}$ can be calculated from equation (4)

The result is

$$\frac{d\Omega}{d\Omega'} = -\frac{4(1+\alpha)^2\cos\phi}{\left[(1+\alpha)^2-\alpha(2+\alpha)\cos^2\phi\right]^2} \tag{14}$$

On using equations (11), (12), (13), (14) the differential cross-section per unit energy becomes

$$\frac{d_e\sigma'(\phi)}{dE_{el}} = \frac{2\pi}{\alpha h\nu}\,k(\theta)\left[\frac{(1+\alpha)^2-\alpha^2\cos^2\phi}{(1+\alpha)^2-\alpha(2+\alpha)\cos^2\phi}\right]^2 \tag{15}$$

FIGURE III

Compton electron distribution for incident gamma-ray energies of 0.511 MeV and 1.28 MeV The dashed curves show these distributions spread out to 10% resolution.

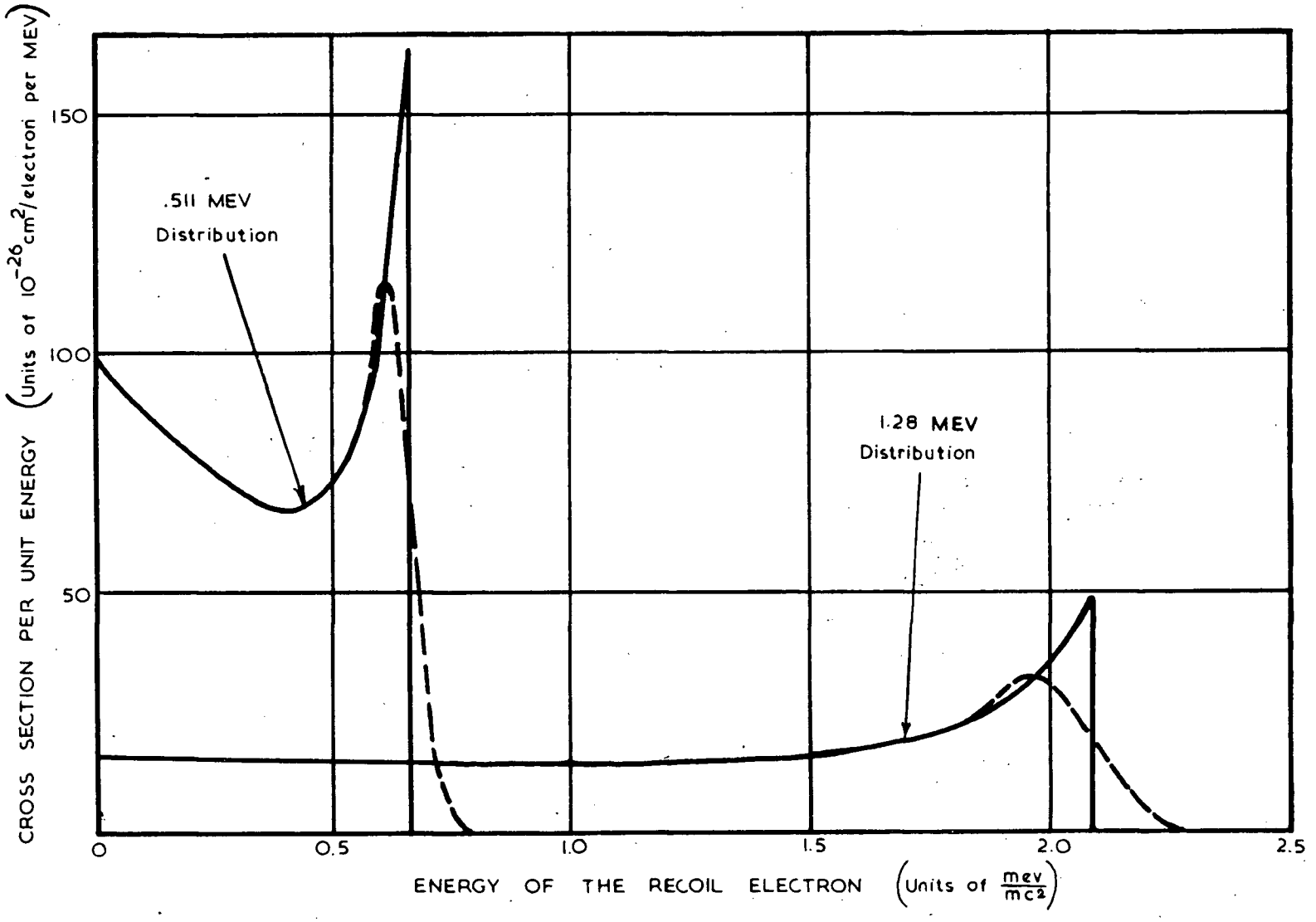

Now, if the energy of the recoil electron is expressed in units of mc^2 i.e. $\alpha_{el} = \frac{E_{el}(MeV)}{mc^2}$

Then equation (15) can be simplified, (See Appendix I) giving

$$\frac{d_e\sigma'(\phi)}{dE_{el}} = \frac{\pi r_o^2}{\alpha^2 mc^2}\left\{2+(\alpha_{el}-2)\left[\frac{\alpha_{el}}{\alpha(\alpha-\alpha_{el})}\right]+\left[\frac{\alpha_{el}}{\alpha(\alpha-\alpha_{el})}\right]^2\right\} \qquad (16)$$

where the maximum energy of the recoil electron is

$$\alpha_{el}(max.) = \frac{2\alpha^2}{1+2\alpha} \qquad (17)$$

Equation (16) has been calculated for the primary quanta energies of 0.511 MeV abd 1.28 MeV (α = 1 and 2.5 respectively). The results are graphed in Fig. (III).

In any experimental case the measured distribution will be spread out due to the finite energy resolution of the system. This spreading of the distribution can be calculated in the following way:

(i) The calculated distribution is divided up into thin vertical strips.

(ii) Each strip is put into the form of a Gaussian of the same area and with a width determined by the resolution of the system

i.e. $\sigma = \frac{E_m R}{2.36}$ where E_m = mean energy of the particular strip

R = resolution of system as defined in the introduction

σ = mean square deviation of the Gaussian.

(iii) The contributions from all the Gaussians are added up

and the resultant distribution plotted.

This has been done for the two distributions mentioned above assuming a resolution of 10% which has been experimentally attained for energies of 1 MeV, and the results are shown in Fig. (III).

In the Compton process, the electron with which the quanta interacts has up till now been assumed to be free. Since the binding energy of the K electron of iodine is approximately 29 KeV, this assumption is no longer valid for incident quanta of energy less than, say, 100 KeV. It would be expected then that there should be considerable modifications to the Compton distribution at these low energies. Since the Compton distribution is rarely observed at these energies due to the overwhelming presence of the photoelectric peak, these effects need not be considered. In general, it has been found experimentally that the Compton distribution is not noticeable until incident quanta energies of several hundred KeV have been reached. In this energy region, and higher, then, the above mentioned effect is negligble.

B. THE PHOTOELECTRIC EFFECT

The medium Z component (iodine Z = 53) of the crystal shows a reasonable photoelectric cross-section for gamma-ray energies up to several MeV. C.M. Davisson has calculated (7) the photoelectric cross-section as a function of energy for various Z absorbers. These calculations are discussed in detail and the accuracy of the results is stated for certain energy ranges. It appears that over the energy range considered the results should be accurate to within 10%.

FIGURE IV

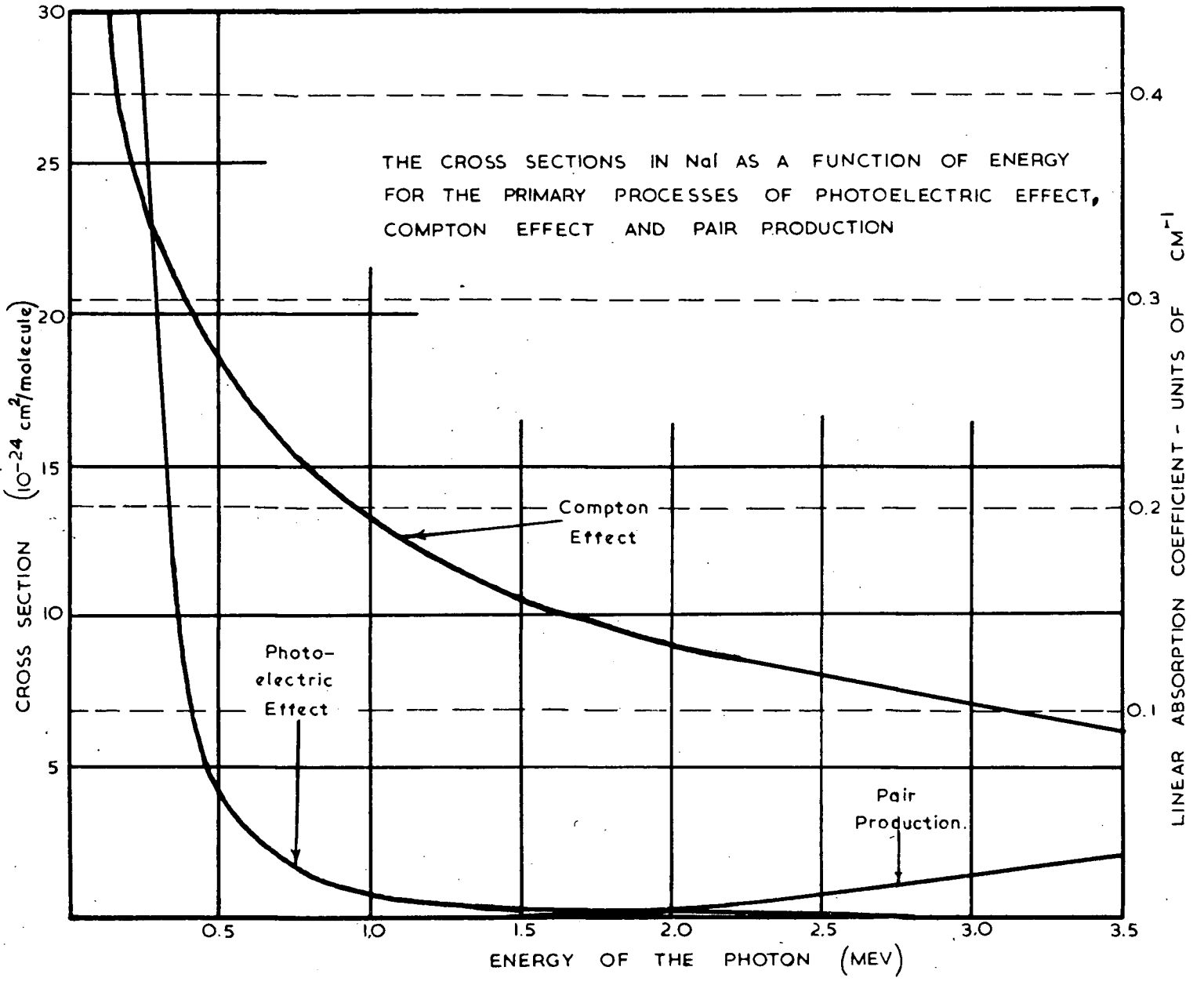
THE CROSS SECTIONS IN NaI AS A FUNCTION OF ENERGY FOR THE PRIMARY PROCESSES OF PHOTOELECTRIC EFFECT, COMPTON EFFECT AND PAIR PRODUCTION
CROSS SECTION (10⁻²⁴ cm²/molecule)
LINEAR ABSORPTION COEFFICIENT - UNITS OF CM⁻¹
ENERGY OF THE PHOTON (MEV)
Compton Effect
Photo-electric Effect
Pair Production.
30
25
20
15
10
5
0.4
0.3
0.2
0.1
0.5
1.0
1.5
2.0
2.5
3.0
3.5

From the tables given in this report the cross-section for sodium iodide at various energies can be calculated. These values are plotted in Fig. (IV). It can be seen from this curve that above 3 MeV the contribution due to the photoelectric effect is negligible.

When spectra of low energy gamma-rays are being investigated it is possible that the gamma-ray energy may go through the K absorption edge of iodine (29 KeV). If this happens, the same considerations apply to the cross-section (i.e. absorption coefficient) as those which apply in the case of X-ray absorption theory, which can be found in any text on X-rays. In effect, then, the crystal just becomes suddenly less efficient when the gamma-ray energy passes through an absorption edge.

In the photoelectric process an electron is ejected from one of the iodine (or sodium) shells, followed by the subsequent emission of an X-ray. The photoelectron presumably loses all its energy to the crystal (neglecting brehmstrahling and edge effects), and the X-ray, due to its low energy, i.e., K X-ray of iodine is 29 KeV, is assumed to be completely absorbed. Consequently, two or more electrons, one of which is the original photoelectron, simultaneously lose energy, where the total energy lost to the crystal must equal the full energy of the gamma-ray. Hence, in effect, the number vs. energy distribution of the photoelectrons can be assumed to be a "line" distribution of effectively zero width, and corresponding to the full energy of the gamma-ray. A "photopeak" should thus occur in the distribution and the position of this peak can be taken as a measure of the energy of the incident gamma-ray.

FIGURE V

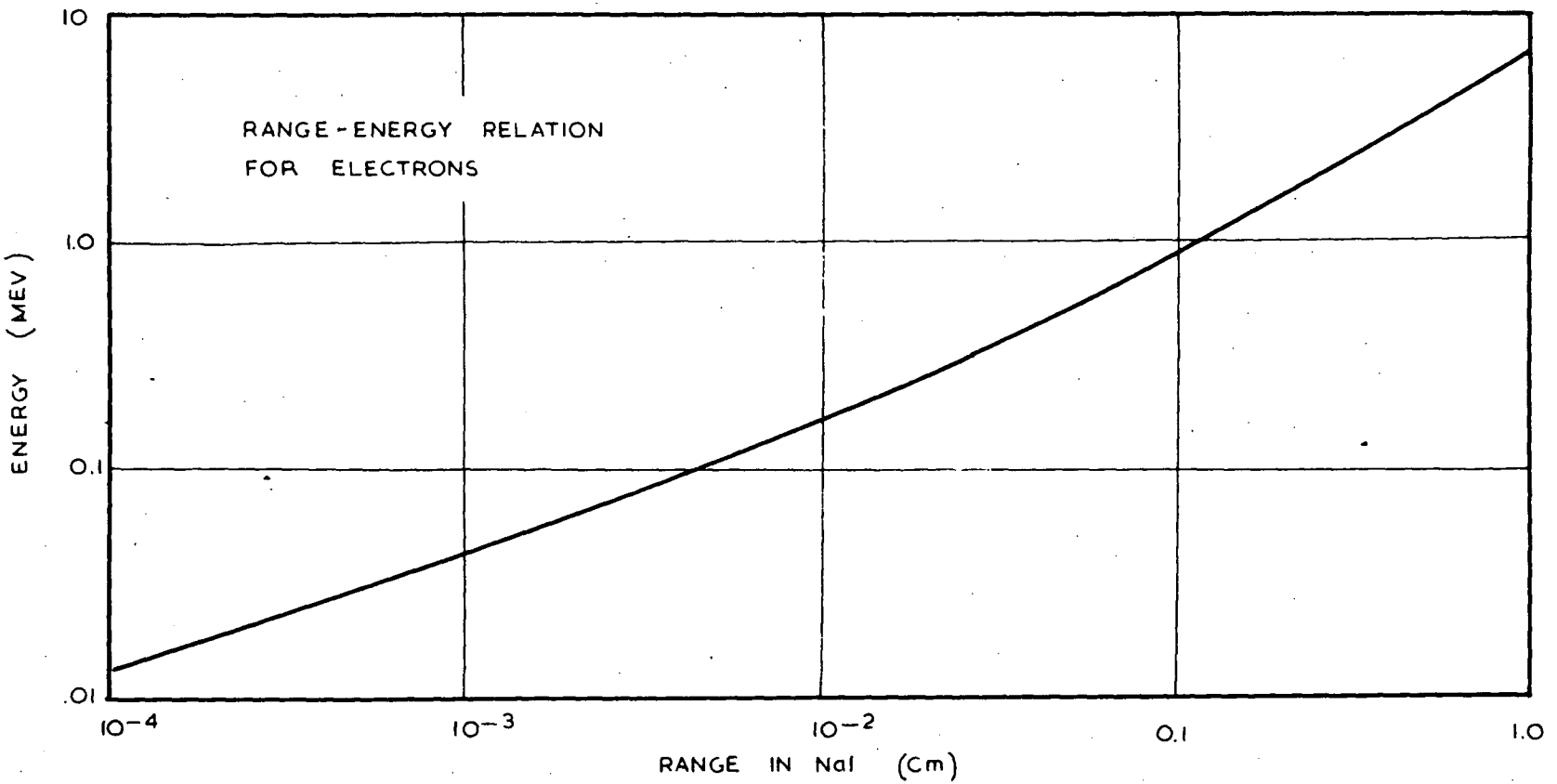
RANGE - ENERGY RELATION
FOR ELECTRONS
ENERGY (MEV)
10
1.0
0.1
.01
10^{-4}
10^{-3}
10^{-2}
0.1
1.0
RANGE IN NaI (Cm)

For a counter with perfect resolution the pulse height distribution from the photomultiplier should be a "line" distribution of zero width. This, of course, is an idealization and hence correction must be made for the finite resolution of the system. This is done by replacing the "line" by a Gaussian of the appropriate width, where the area under the Gaussian (i.e., the total number of photoelectrons produced) is compatible with the photoelectric cross-section at the given energy. That the actual photopeak is Gaussian has been verified by experiment.

If the crystal dimensions are very small, then the probability of escape of the iodine X-rays is no longer negligible. An "escape peak" should then appear in the distribution with energy equal to the difference between the energy of the incident quanta and of the X-rays of iodine.

With a very thin crystal it might also be possible to have a peak at 29 KeV which would result if many of the photoelectrons escaped completely from the crystal while the X-rays of iodine were absorbed. However, due to "straggling" in the wall effect and the fact that the above sequence of events is not too probable, this effect may be neglected. No peak at 29 KeV has yet been observed by the author, although escape peaks have.

The magnitude of the wall effect depends on two factors:

1) The range in NaI of the photoelectrons.

2) The dimensions of the crystal.

The range vs. energy curve for the electrons has been calculated from Feather's rule and is shown in Fig. (V). Mateosian and Smith (8) have outlined a method for calculating the wall effect

but due to the nature of the experiments so far performed by the author it has not been found necessary to make this calculation.

C. PAIR PRODUCTION PROCESS

At energies greater than 2 mc^2, i.e., greater than 1.02 MeV, absorption of gamma-rays by the process of pair production occurs. The cross-section at different energies for this process in sodium iodide can be calculated from the tables published by Davisson (7). A graph of these values is shown in Fig. (IV).

The absorption of energy by the crystal due to pair production occurs in the following manner:

Consider an incident quantum of energy E_γ MeV

(i) The quantum annihilates, producing an electron-positron pair whose total kinetic energy is E_γ -1.02 MeV. Both positron and electron are assumed to lose all their energy to the crystal.

(ii) The positron then annihilates with an electron, producing two quanta each with energy 0.511 MeV.

(iii) Both the annihilation quanta may be absorbed by the crystal, only one may be absorbed with the other escaping, or both may escape from the crystal.

Hence, three peaks, designated Pair I, Pair II, and Pair III should appear in the spectrum with energies corresponding to E_γ (both annihilation quanta captured), E_γ - 0.511 MeV (only one annihilation quantum captured) and E_γ - 1.02 MeV (both annihilation quanta escape) respectively. These peaks are ideally zero width peaks, but due to the finite resolution of the counter they are subjected to the same conditions of broadening as was indi-

cated for the photoelectric peaks.

The relative heights of the three pair peaks depend critically on the dimensions of the crystal. These relative heights cannot be calculated exactly as a function of crystal dimensions but qualitatively, at least, some estimation can be made. For example, consider a cylindrical crystal whose dimensions are 3 cm. in diameter and 3 cm. in length. Now if it is assumed that all pairs are produced and annihilate somewhere along the axis of the crystal or very close to it, (this is a fair assumption for incident quanta energies up to 2 or 3 MeV and for good collimation) then for an order of magnitude calculation it may be assumed that all annihilation quanta have a 1.5 cm. path length on the average before escaping from the crystal. Suppose it is further assumed that if an annihilation quantum suffers one scattering event in the crystal that it is then completely absorbed, otherwise it escapes completely. For a .511 MeV quantum the absorption coefficient in NaI is 0.34 cm^{-1}. From this value and the above assumptions the following probabilities for a pair of annihilation quanta can be found:

(i) Probability that both quanta escape = 0.36

(ii) Probability that only one quantum escapes = 0.48

(iii) Probability that both quanta are absorbed = 0.16

Hence for these conditions the three pair peaks should be in the ratio

Pair III : Pair II : Pair I = 0.36 : 0.48 : 0.16

These three peaks, where the total area under them must be compatible with the cross-section at the given energy, are superimpos-

FIGURE VI

Calculated pulse height distribution for the 2.62 MeV gamma-ray of RdTh assuming all annihilation quanta escape. A resolution of 8% was assumed in the calculations.

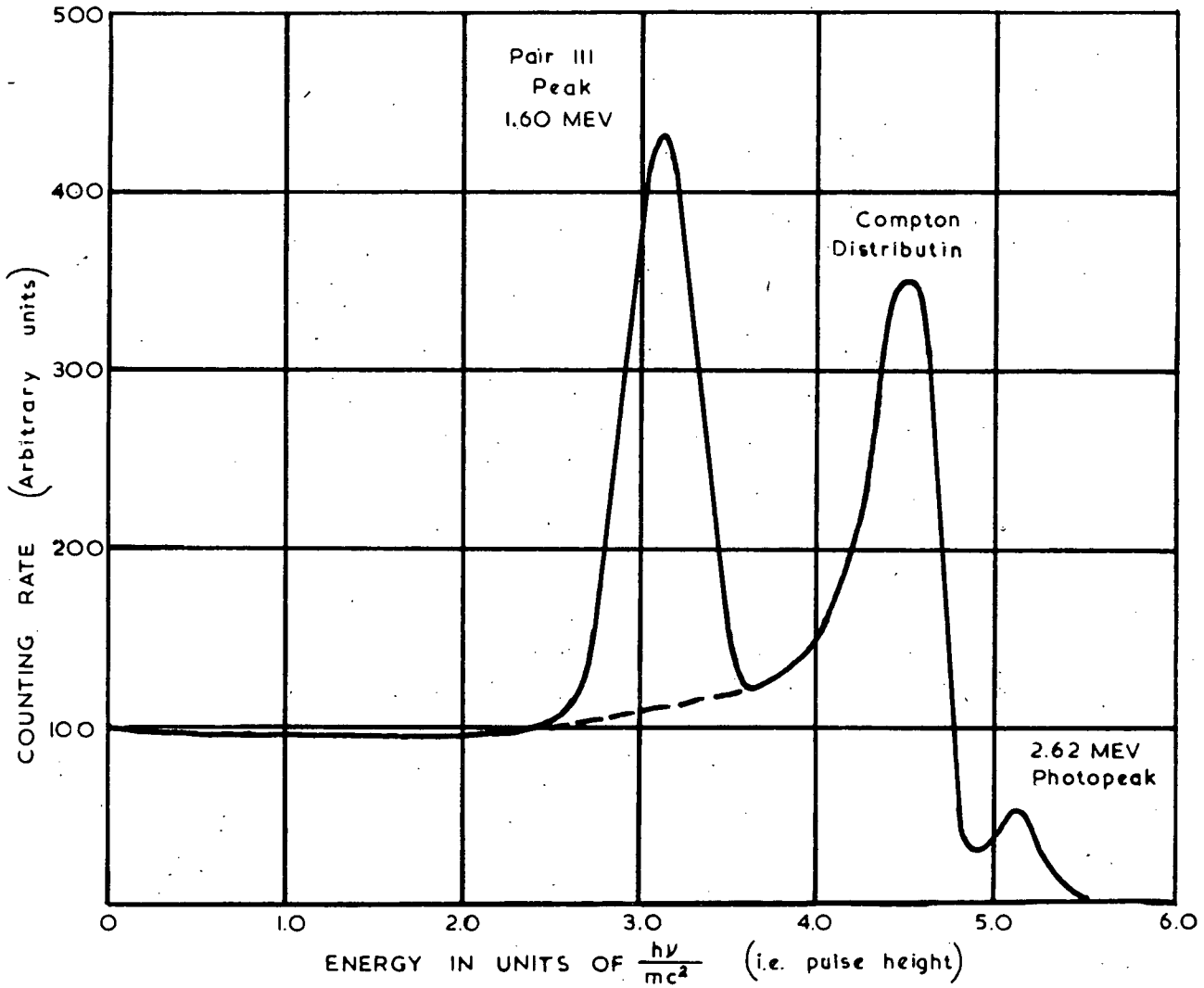

ed upon the Compton and photoelectric distributions to give the resultant distributions. At 0.511 MeV the absorption is mainly by the Compton process, so that due to multiple scattering of the absorbed annihilation quanta, it would be expected that there would be considerable broadening of the Pair I and Pair II peaks. At high energies (e.g., > 10 MeV) further broadening effects would result from losses by brehmstrahling and by wall effects.

The rough calculations presented above show that the dimensions of the crystal are the most significant factor in determining precisely the distribution due to pair production. An increase in overall dimensions will make Pair I and Pair II the dominant peaks, and for very large dimensions only Pair I should be significant. For very small crystals (i.e. "disc" crystal) only Pair III would be significant, but in this case wall effects are very important and considerable spreading of the distribution due to this effect would be probable. Since no rigorous calculation has been made for the relative heights of the three peaks the only diagram on the pair process Fig. (VI) is constructed assuming that only the Pair III peak occurs (i.e. limiting case for small crystals).

D. THE CALCULATED SPECTRUM SHAPE

It has been shown that, assuming primary events only, and neglecting other broadening effects each of the absorption processes give rise to a characteristic pulse height distribution. The relative number of pulses for a given gamma-ray energy due to each process can easily be found from their relative cross-sections, i.e., the ratio of the areas under the distributions must

FIGURE VII

Calculated pulse height distributions for gamma-ray energies 0.511 MeV and 1.28 MeV. The curves calculated assuming primary processes only and a resolution of 10%.

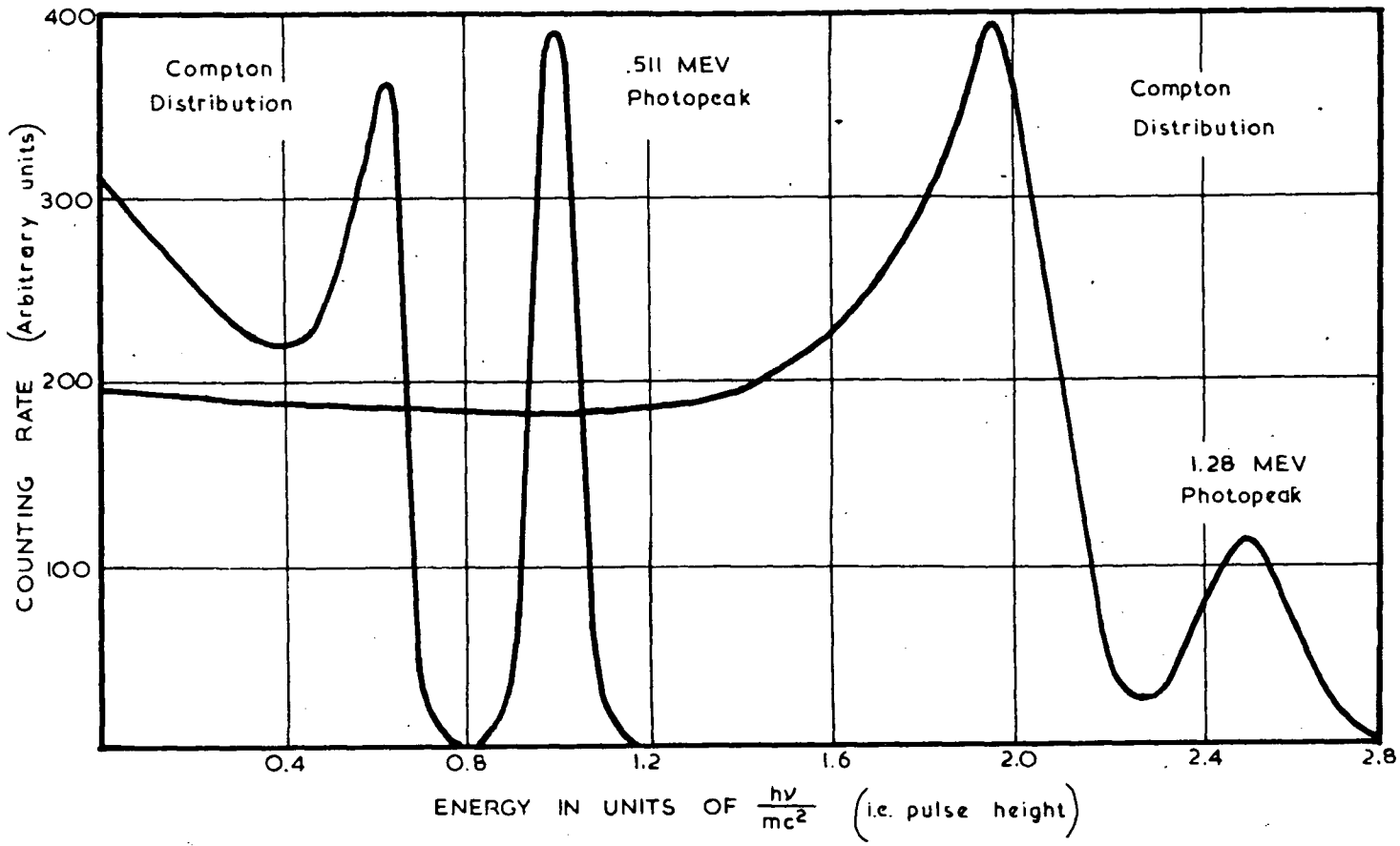

FIGURE VIII

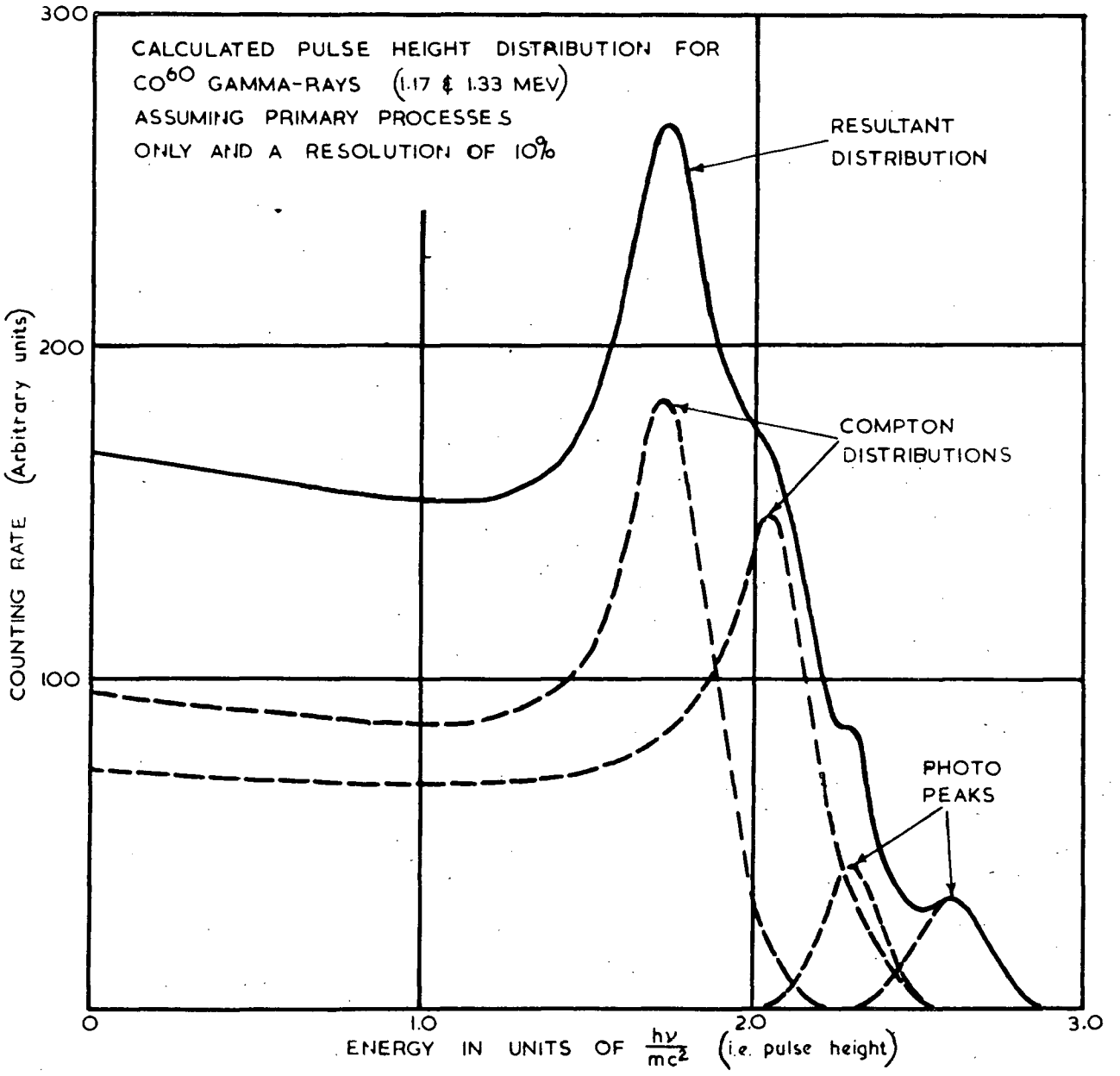
CALCULATED PULSE HEIGHT DISTRIBUTION FOR
CO60 GAMMA-RAYS (1.17 & 1.33 MEV)
ASSUMING PRIMARY PROCESSES
ONLY AND A RESOLUTION OF 10%
RESULTANT
DISTRIBUTION
COMPTON
DISTRIBUTIONS
PHOTO
PEAKS
COUNTING RATE (Arbitrary units)
300
200
100
0
1.0
2.0
3.0
ENERGY IN UNITS OF hν/mc² (i.e. pulse height)

be equal to the ratio of the cross-sections. On this basis, the expected pulse height distribution has been calculated for incident gamma-ray energies of 0.511 MeV, 1.28 MeV, and 2.62 MeV. The first two distributions were calculated assuming 10 percent resolution, and the third assuming 8 percent resolution. These distributions are shown in Fig. (VI) and (VII). The pulse height distribution for the Co^{60} gamma-rays (1.7 and 1.33 MeV in cascade) has also been calculated, assuming 10 percent resolution, and is shown in Fig. (VIII).

The calculated distributions mentioned above hold only in the limiting case of very small crystals. As the crystal dimensions are increased these distributions will only be an approximate indication of the shape. The effects of crystal dimensions and multiple scattering will be considered in the next section.

E. MULTIPLE SCATTERING

Figures (VI), and (VII), and (VIII) show the spectrum shape calculated on the assumption that multiple scattering events do not occur. This assumption is identical to the assumption that the crystal is very small. Since experimentally, the crystals are of finite dimensions, it can be expected that with increasing dimensions multiple scattering events will become more prominent.

Multiple scattering events play a negligible role in the distribution from the photoelectric effect (aside from the possibility of an escape peak and a 29 KeV peak mentioned earlier). If brehmstrahlung is construed as a multiple scattering event, then at high energies this effect will become appreciable, and pulses

will be lost from the photopeak due to escape of brehmstrahlung radiation. This effect can be neglected except at fairly high energies. (>10 MeV)

The presence of three peaks in the pair production distribution has been demonstrated previously. The dependence of the relative heights of these peaks on the dimensions of the crystal has been indicated but no quantitative estimations have been made.

The largest contribution to multiple scattering comes from the Compton process where a secondary quantum is produced in every collision. Qualitatively, it would be expected that many pulses from the region of the Compton peak will be transferred to the photopeak due to the capture of the soft back-scattered quanta. For example, again consider a cylindrical crystal 3 cm. in diameter and 3 cm. in length and a collimated beam of, say, 1.28 MeV gamma-rays incident upon it. The back-scattered quanta will be of the order of 300 KeV. Assume that all these quanta originate uniformly along the axis of the crystal, (this assumption is valid within the accuracy desired since the half thickness in NaI for 1.28 MeV gamma-rays in 4.3 cm.) and that the average escape path length of the quanta is 1.5 cm. Then from the absorption coefficient 0.6 cm^{-1} for 300 KeV quanta see Fig. (IV) approximately 60% of the back-scattered quanta are absorbed, mostly through the photoelectric process. On this simple calculation it would be expected that approximately 60% of the pulses in the Compton peak would be shifted upwards to some extent. All other quanta which are scattered in a direction other than back will be subject to the same considerations but with a correspondingly smaller ef-

fect. Consequently, the photopeak will have added to it very many pulses from the Compton distribution. Experimentally it has been found that the photopeak is much larger than the cross-section would indicate, where the increase is roughly in agreement with the above calculations. These results will be described later in the section on experimental results.

It is quite obvious from these arguments that there are two limiting cases:

(i) Very small crystals where all degraded quanta escape. These calculations have been carried out explicitly in the preceding sections.

(ii) Very large crystals where all the degraded quanta are completely absorbed and the resultant distribution consists of only one peak corresponding to the full energy of the incident gamma-ray.

As the crystal dimensions are varied from very small to very large between these two limits, the ratio of Compton peak height to photopeak height should decrease steadily to zero. The crystal dimensions which give the best resolution cannot be predicted unless the above calculations are carried out exactly. These dimensions are determined experimentally as will be described in the section on experimental results.

Whenever possible, experiments have been done using a precisely collimated beam to reduce the broadening effects of multiple scattering. It is quite easy to see how an uncollimated beam would result in very poor resolution by assuming in the argument above that scattered quanta could originate at any point within the cry-

stal. R. Hofstadter (2) has demonstrated very forcibly the effect of collimation on the resolution.

F. RESOLUTION OF THE SCINTILLATION COUNTER

The statistical spread in the pulse height distribution of a scintillation counter is influenced by the following factors:

(i) The number of photons emitted by the phosphor.

(ii) The number of photons transmitted to the photocathode.

(iii) The quantum efficiency of the photocathode.

(iv) The number of photoelectrons reaching the first dynode.

(v) The secondary emission ratio of the dynodes.

Each of these factors has associated with it a statistical uncertainty. P.W. Roberts has deduced an expression (9) which gives the spread of the distribution due to these uncertainties. This expression is

$$\sigma^2 = \frac{1}{N}\left(\frac{\delta_0^2}{N} - 1\right) + \frac{1}{N f p q}\left[1 + \frac{\delta_1^2}{m_1^2} + \frac{\delta^2}{m_1 m (m-1)}\right] \qquad (1)$$

where σ^2 = fractional variance in pulse height distribution

N = number of photons emitted by the phosphor

δ_0^2 = variance of N

m_1 = gain of the first stage

m = gain of each succeeding stage

δ_1^2 = variance of the secondary emission ratio of the first stage

δ^2 = variance of the secondary emission ratio of each succeeding stage

variance = (standard deviation)^2

f = fraction of photons transmitted to the photocathode

p = quantum efficiency of the photocathode

q = fraction of photoelectrons which reach the first dynode

A binomial distribution was assumed in calculating the effects of the factors f, p, and q, and the expression has been approximated to the case of a large number of dynode stages.

Equation (1) can be rewritten

$$R^2 = 5.6\left(A + \frac{B}{nE}\right) \tag{2}$$

where $R^2 = \left(\frac{\text{width of peak at half max. (MeV)}}{\text{energy of peak (MeV)}}\right)^2 = (2 \times 1.18\sigma)^2$

The numerical factor is that one which converts the standard deviation of a Gaussian into the full width at half maximum.

$$A = \frac{1}{N}\left(\frac{\delta_0^2}{N} - 1\right)$$

$$B = \left[1 + \frac{\delta_1^2}{m_1^2} + \frac{\delta^2}{m_1 m(m-1)}\right]$$

E = energy of peak in MeV

$n = \frac{Nfpq}{E}$ = number of photoelectrons per MeV reaching the first dynode

If the number of photons per MeV produced by the incident gamma-ray is assumed to follow a Poisson distribution then the term A becomes zero. However, A has been found to be non-zero, in most cases, but very small, so it is left as a parameter to be determined by experimental results. This term, then, represents the spread of the distribution due to non-uniform response of the crystal.

Since the term A has been found to be very small, the second term only of equation (2) need be considered.

Then $R^2 \approx 5.6 \frac{B}{nE}$

If the photomultiplier gain per stage is assumed to be 3, then B is approximately 4/3.

For an incident energy, say, of 1 MeV

$$R^2 \approx \frac{7.5}{n}$$

It is quite obvious that n, the effective number of photoelectrons produced at the photocathode per MeV, determines the ultimate resolution attainable with the counter.

e.g. if n = 500 then R $\approx$ 12.2%

if n = 1000 then R $\approx$ 8.7%

For a given crystal and photomultiplier tube the only factor of which can be increased is f, the fraction of the photons which reach the photocathode. It is essential, then, that efficient crystal mounting$ techniques are developed.

III. CRYSTAL MOUNTING TECHNIQUES

It has been shown that the largest single gain in resolution, aside from improved crystals and photomultiplier photocathode efficiencies, can be obtained by improved crystal mounting techniques. Considerable work has been done on improving the efficiency of light collection of the mounts.

Sodium iodide crystals are very deliquescent, the surfaces immediately becoming discoloured on contact with the water vapour in the atmosphere, so that any mount designed for the crystal must provide perfect protection against water vapour. The original method of mounting used by the author consisted of immersing the crystal in a clear, water free, mineral oil in a light tight aluminum container. This container was highly polished on the inside, and the oil contact between the crystal and the container provided the necessary optical coupling for optimum reflection efficiency. The oil film also acted as a preservative for the optical properties of the crystal surfaces. The resolution obtained with mountings of this type was never very good.

For mountings of this type Gillette has shown (10) that the entrapment of light due to Fresnel reflections constitutes a very serious loss in the transmission of light to the photocathode. It is also shown that the transmission is increased many times by using some form of diffuse reflection at the surfaces of the crystal. Consequently, a method of crystal mounting was sought which provided this necessary property.

R.K. Swank has reported (5) a method of mounting crystals

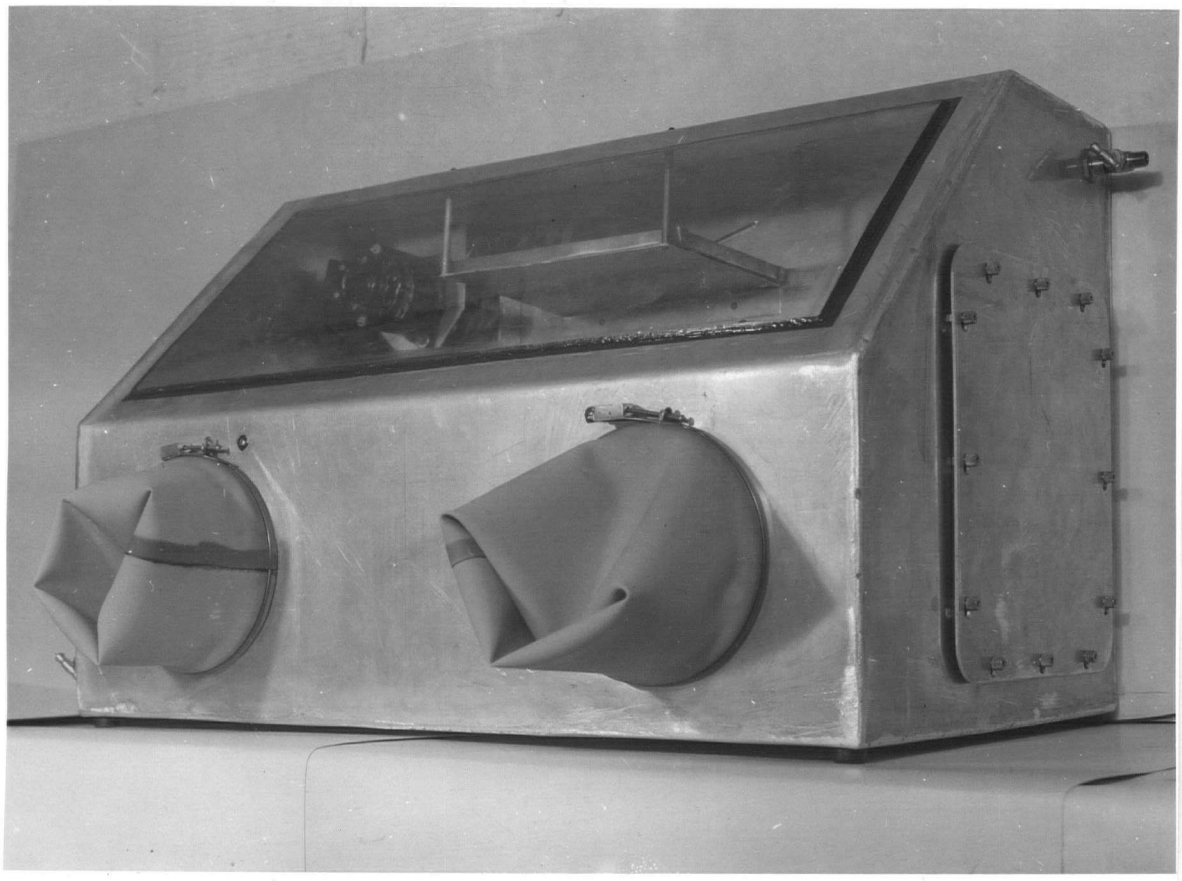

PLATE I

THE DRY BOX

using the highly efficient, diffuse reflecting properties of powdered magnesium oxide. This method requires that the crystals be mounted dry (i.e., completely free from all traces of oil in which they are stored) since the reflecting properties of the magnesium oxide are destroyed if the powder becomes "matted" with oil. This has made the design and construction of a "dry box" necessary so that all mounting operations can be carried out in a dry atmosphere, thus preventing the surfaces of the crystal from being discoloured due to contact with moisture. The magnesium oxide, itself, is slightly deliquescent so that it must be baked for several hours at about 500°C before it is used.

A. THE DRY BOX

The "dry box" is a large metal box, of dimensions 30" wide x 18" deep x 20" high. It has a sloping front window 27" x 11" made of plexiglass. Construction is of aluminum sheet throughout, all joints are butt welded, and the whole enclosure is made air-tight. An air-tight door is provided on one side of the box to permit materials to be conveniently placed inside. Illumination is provided by a small, 15 watt fluorescent tube inside the box. The box contains a flat, removable tray 8" long x 11" wide x 1/2" deep in which is placed a mixture of sand and phosphorous pentoxide as the drying agent. A small air blower is so located that the atmosphere within the box is continually circulated over the drying agent. A Moisture indicator is placed inside the box. Two valves are supplied, one on each end of the box, so that a continuous flow of dried nitrogen may be passed through the box. This

~~This~~ serves the purpose of sweeping out any organic vapours which may have accumulated due to the final crystal polishing process carried out inside the box. This is necessary since the surfaces of the crystal quickly become clouded on contact with most organic vapours.

Work is done in the box through long sleeve rubber gloves which enter through glove ports in the front panel. The ends of the gloves are attached to these ports by an airtight seal, but may readily be removed and replaced.

The details of construction of the box are shown in Plate I .

B. CRYSTAL MOUNTS

The mounting for a sodium iodide crystal must satisfy the following three requirements:

(1) The gamma-rays must enter the crystal with little absorption or scattering.

(2) The fluorescent light must be extracted with a uniformly high efficiency from all parts of the crystal.

(3) The mount must be light tight and impervious to water vapour.

(4) Optical coupling to photocathode of photomultiplier must be good.

In addition, such obvious requirements as ruggedness and insensitivity to orientation and temperature variations must be met.

The final design, with which most of the results have been obtained, consisted of an aluminum container with a lucite window. Sufficient space is left between the crystal and the container so

FIGURE IX

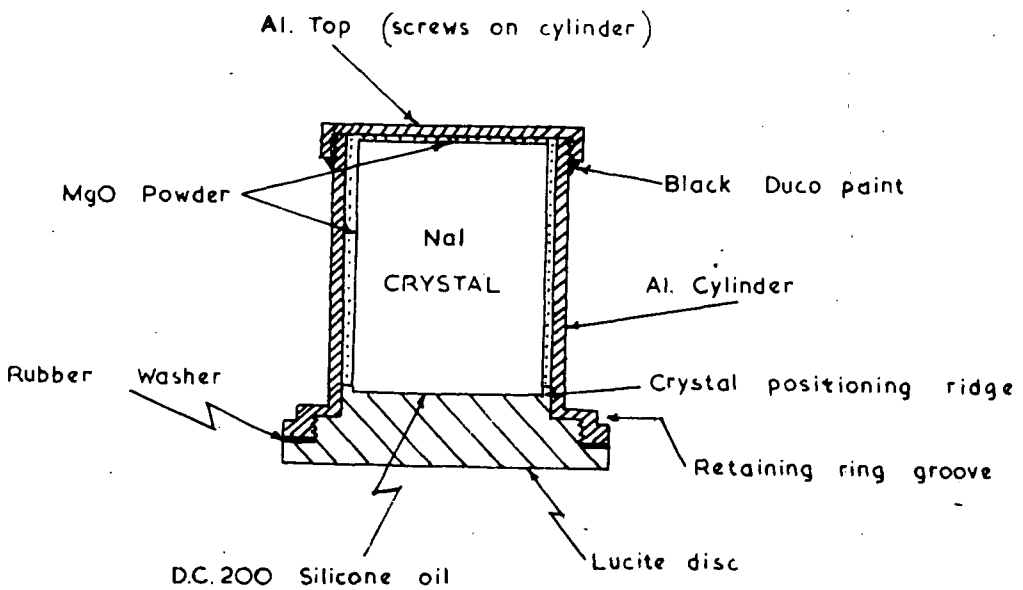

Mount for the cylindrical crystal drawn to scale. The mount is optically coupled to the photomultiplier tube with D.C. 200 silicone oil, and held in place by a ring which fits in the retaining ring groove.

FIGURE X

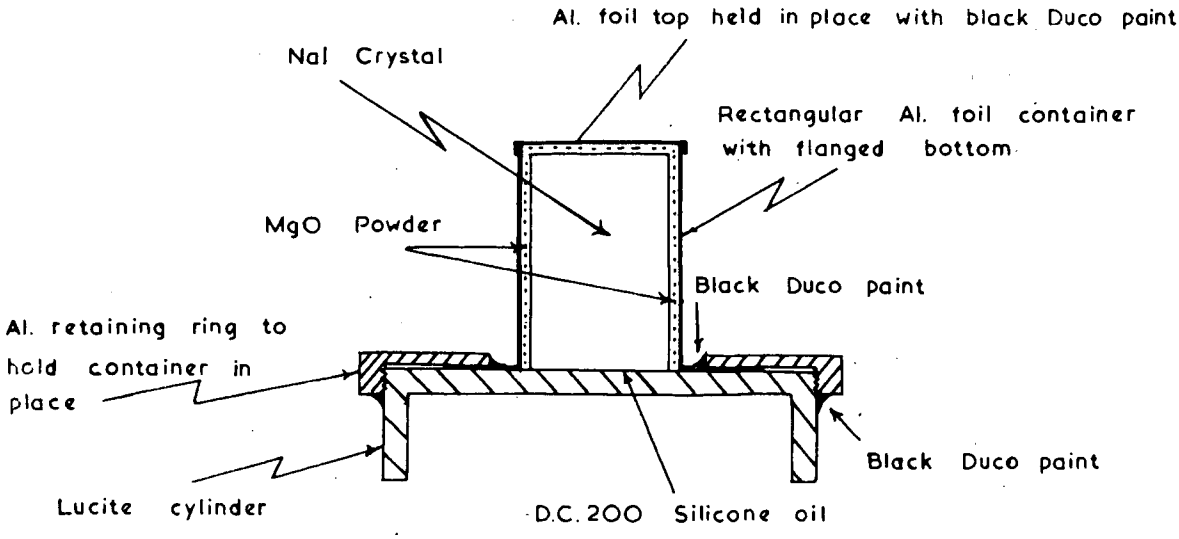

Mount for the rectangular crystal drawn to scale. The mount is attached to the photomultiplier tube with black electrical scotch tape using D.C. 200 silicone oil for optical coupling.

FIGURE XI

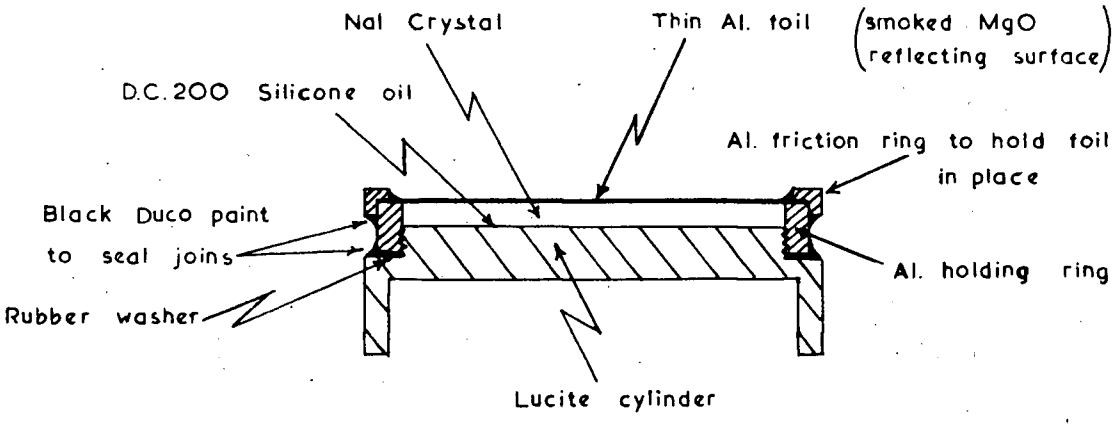

Mount for the thin cylindrical crystal drawn to scale. The mount is attached to the photomultiplier tube with black electrical scotch tape. Any places which may leak light are painted with black Ducco paint.

that powdered magnesium oxide may be packed in to form a reflecting surface. The crystal is optically coupled to the lucite window by the use of D.C. 200 (Dow Corning) silicone oil (10^6 centistokes viscosity). Movement of the crystal is prevented by a lucite positioning ring (in mounts for cylindrical crystals only) and by tight packing of the assembly.

This basic design has been adapted for mounting three types of crystals:

(1) Cylindrical crystals.

(2) Rectangular crystals.

(3) Thin "wafer" crystals.

The details of the design of the mounts for each type of crystal are shown in Fig. (IX), (X), and (XI) respectively. Data particular to each design are shown on the Figures.

C. DETAILS OF TECHNIQUE

All rough polishing of the crystal is done outside the dry box. This is carried out by using white blotting paper soaked in acetone as the abrassive surface. After being rubbed on this surface several times the crystal is transferred to a piece of blotting paper soaked in mineral oil on which it is rubbed to remove all traces of acetone. This process is repeated several times until the surfaces of the crystal are quite clear. The crystal is then placed in a bath of mineral oil to preserve its surfaces. It is then transferred to the dry box, along with the other thoroughly dried out components. A two hour "drying-out" time is allowed so that the atmosphere within the box can become thoroughly

dry. The crystal is then removed from its oil bath, its surfaces wiped completely free of all traces of oil, and if necessary is given a final polishing. This is done by "dry" polishing the crystal on blotting paper. It has seldom been found necessary that further polishing with organic solvents is required once the crystal is placed in the dry box. However, provision is made in case this is necessary. After the final polishing, the mounts are assembled, and any joins in the mount which may leak moisture into the crystal are covered with a thin layer of paraffin wax. These joins are then painted over with black "Ducko" paint to form a permanent join. The mountings are then removed from the box and attached to the photomultiplier tube, using D.C. 200 silicone oil as the optical couple. With this ~~arrangement~~ technique and the dry MgO, crystals remain clear and the ~~performance~~ has not varied over a three month period.

IV. THE GAMMA-RAY SPECTROMETER

It has been shown (11) that a pulse amplitude distribution curve obtained with a differential analyzer is subject to a smaller statistical uncertainty than the curve obtained by differentiating an integral bias curve. Hence, the simplest differential analyzer was used for this work, a "Single Channel Kicksorter", in which only those pulses which lie above a "baseline" voltage and within a "window" immediately above it are counted. Either the baseline and window voltages can be adjusted separately, or as is usual for most of the work of this type, it is more convenient to set the window width and shift the baseline.

There are two main types of experiments which can be done with this equipment:

(a) Experiments involving bombardment of target materials with accelerated particles in which case one has to use either the integrated target current as a monitor, or a separate gamma-ray monitor as a reference, or perhaps both.

(b) Experiments involving the measurement of gamma-ray spectra from radioactive sources of reasonably constant or slowly decaying activity.

Most of the author's work consisted of experiments of the type (b). For this purpose the baseline of the kicksorter was driven at a constant rate (with a fixed window width) by a synchronous motor through a system of gears. The gear system is so designed that three driving speeds are possible (1 volt/36 sec., 1 volt/1 min. 12 sec., 1 volt/6 min.). The kicksorter output pulses are fed

FIGURE XII

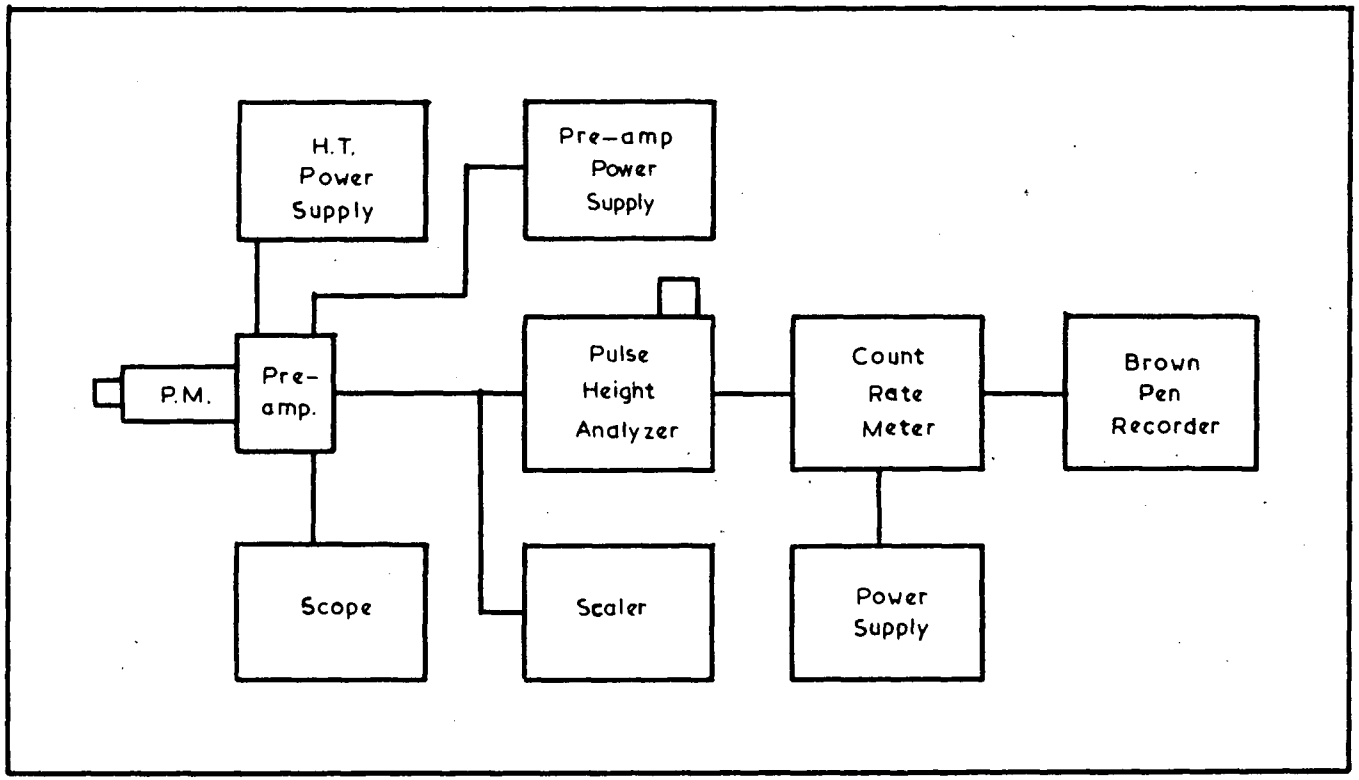

BLOCK DIAGRAM OF THE SPECTROMETER

FIGURE XIII

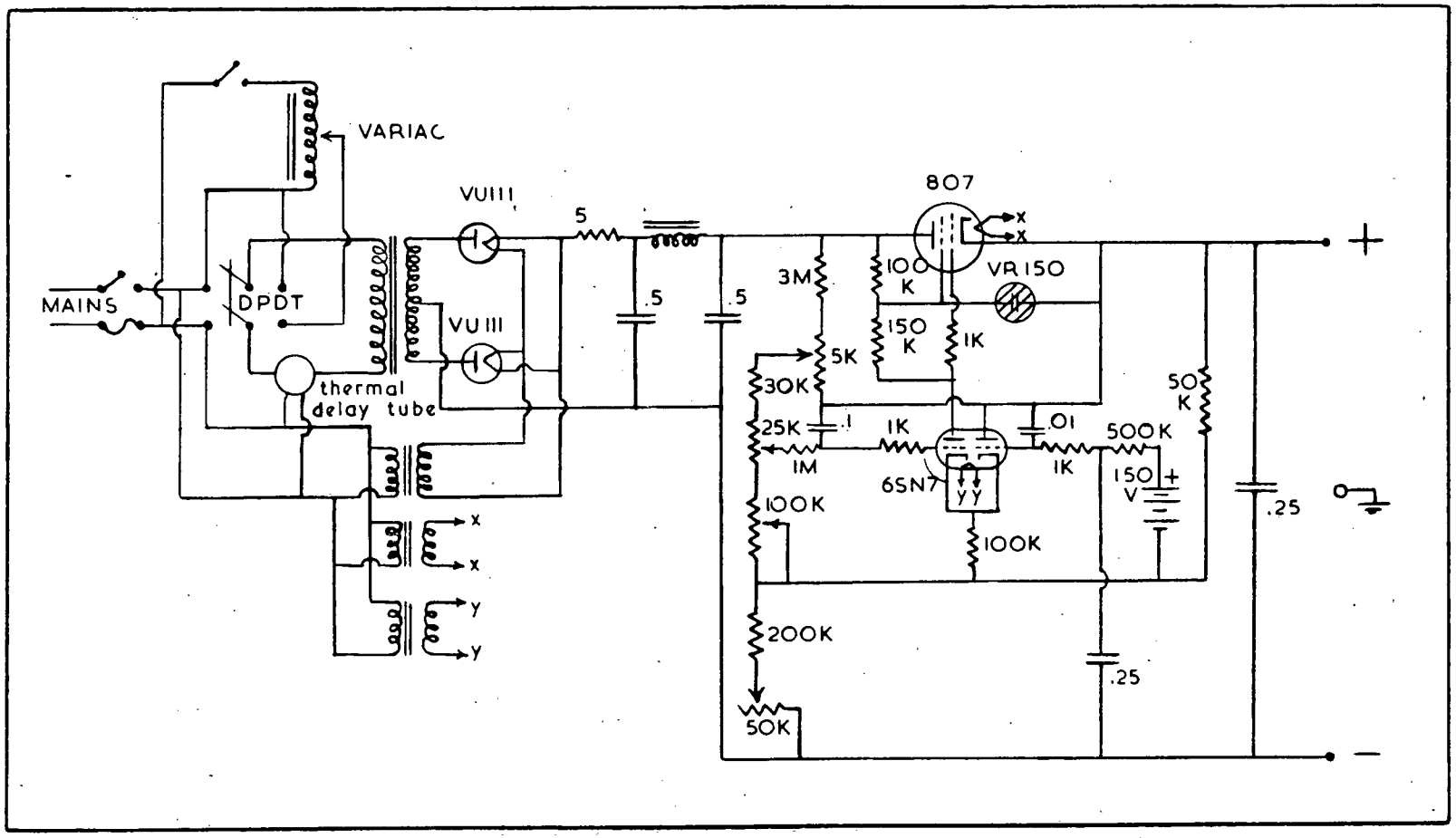

H.T. POWER SUPPLY
2500 V. MAX.

into a linear count rate meter, and the counting rate is recorded on a "Brown" recording potentiometer. A block diagram of the system is shown in Fig. (XII).

It has been found that for this method to give reliable results the lowest counting rate (for a given channel width) that could be tolerated was of the order of 10 counts per second. In any experiment the window width was set so that this minimum counting rate was always exceeded, with the added condition that the narrowest peak in the distribution should be at least three channels wide. Measurements involving very weak intensities cannot be done by this "continuous drive" method, and for these cases manual operation of the kicksorter would be necessary.

A description of each element of the spectrometer, along with the operating characteristics are given below.

A. H.T. POWER SUPPLY

The gain of the photomultiplier tube is very sensitive to the voltage applied across it. In the type of tube used (E.M.I. type 6262) the gain was found to increase by 50 percent for a voltage change of 50 V. Consequently, a voltage supply of exceptionally long term stability is required. A supply has been constructed whose measured long term stability was better than 0.1 percent. The supply is electronically stabilized using a 150 V. battery as reference and is capable of delivering 10 milli-amps. at 2000 volts. The circuit diagram is shown in Fig. (XIII).

B. COUNT-RATE METER AND HEAD AMPLIFIER POWER SUPPLIES

Both these supplies are commercially built units obtained from the "Lambda Electronics" Corporation, and are designated "Model 28". A negative "rail" capable of delivering 10 milli-amps. at minus 150 volts has been built into each unit. Both these supplies, and the H.T. supply are driven from a constant-voltage mains transformer.

C. OSCILLOSCOPE

A model 511D "Tetronix" oscilloscope was used for investigating pulse shapes and sizes at various points in the circuit. No quantitative measurements were made with it, and it was used solely for convenience in "setting up" the apparatus.

D. THE PHOTOMULTIPLIER TUBE

An E.M.I. type 6262 fourteen stage multiplier was used for all the experiments. The tube was operated between 1000V and 1400V depending on the spectra being investigated. The noise background was found to be negligible at all voltages, but when measurements on gamma-rays of energy less than 10 KeV were attempted the noise becomes overwhelming. The maximum gain of these multipliers is of the order of 10^9, and the output was found to be linear for pulses up to 30 volts at least. The signal was taken from the last dynode and not the final collector since a positive pulse was required to drive the analyzer.

E. THE PRE-AMPLIFIER

The pre-amplifier consists of a cathode follower stage only

FIGURE XIV

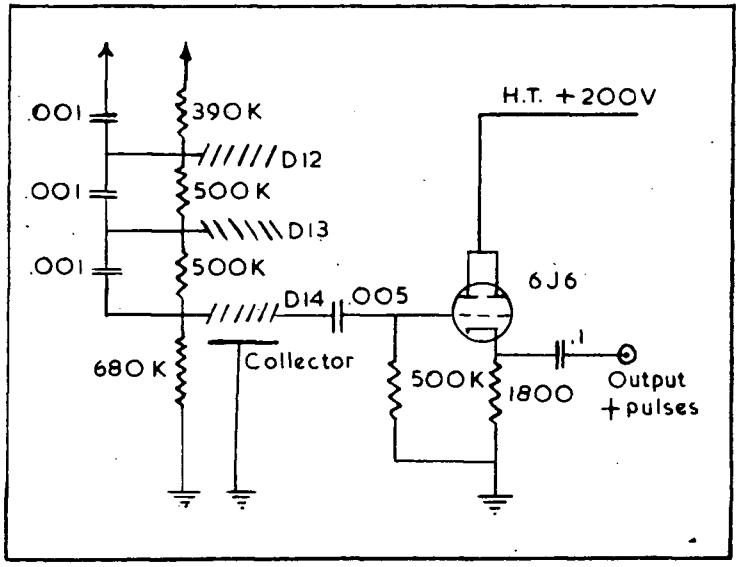

PRE-AMPLIFIER

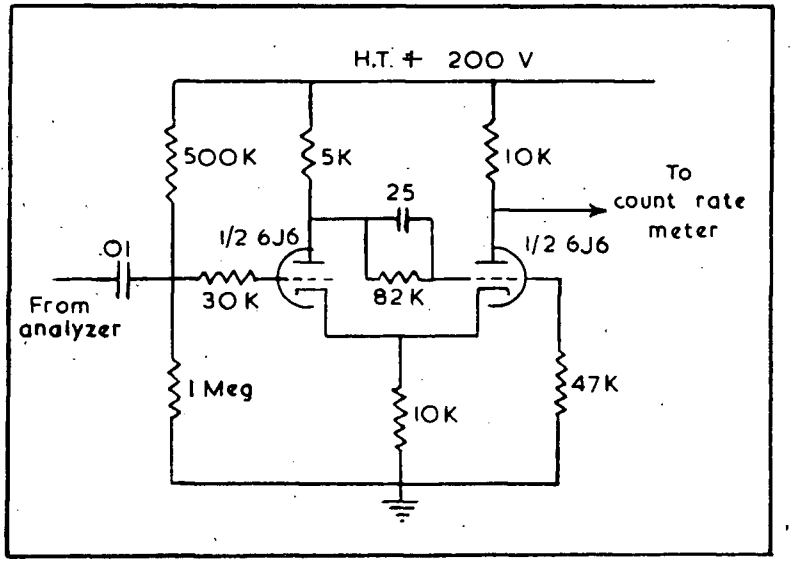

SCHMITT CIRCUIT INPUT TO COUNT-RATE METER

(see Fig. (XIV)) for feeding into a 100 ohm line. No amplifier stage was included since it was felt that the pulses available from the photomultiplier tube were sufficiently large for analyzing purposes.

F. THE SINGLE CHANNEL ANALYZER

The analyzer is a commercially built unit supplied by the Atomic Instrument Company, and designated "Model 510". The operating characteristic are given in the pamphlet entitled "Interim Instruction Manual, Model 510 Single Channel Pulse Height Analyzer" obtainable from the Atomic Instrument Company. The operating characteristics of the analyzer were found to be quite adequate for handling the pulses obtained from a NaI(Tl) scintillation counter (rise time $\approx$ 0.25 sec). The analyzer is capable of handling pulses up to 100 V maximum, and has a maximum window width of 7.5 V. The maximum pulse input rate is 2500 c.ps. (for 5% loss).

G. THE COUNT RATE METER

Elmore and Sands (12) give the theory of the operation of a count rate meter. A discussion of the linearity is given and an expression is deduced for the fractional probable error in the counting rate. This expression is $\epsilon = 0.67 \frac{1}{\sqrt{2 n RC}}$

where n = average counting rate

RC = integrating time constant

Cooke-Yarborough has designed (13) a count rate meter which uses a 100% feedback D.C amplifier to ensure linearity. A model was built to this circuit and found to be linear to better than

FIGURE XV

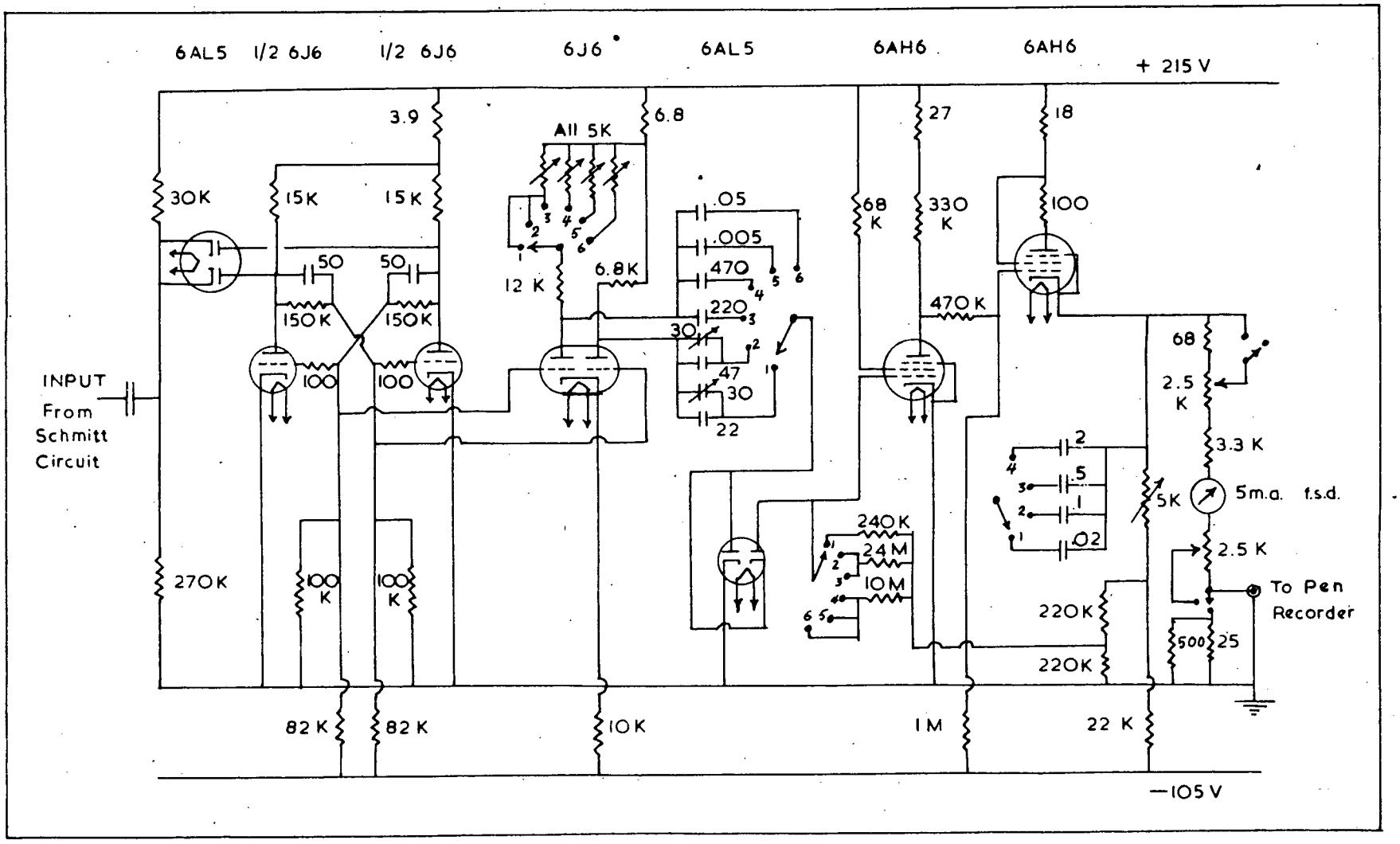

COUNT RATE METER

TABLE I

Counting Rate f.s.d.	Time Constant (Sec)	% P.E. at Half Scale deflection
10^5 c.p.s.	4.8×10^{-3}	3.0
	24×10^{-3}	1.5
	120×10^{-3}	0.6
	480×10^{-3}	0.3
10^4 c.p.s.	48×10^{-3}	3.0
	240×10^{-3}	1.5
	1.2	0.6
	4.8	0.3
10^3 c.p.s.	48×10^{-3}	10.0
	240×10^{-3}	5.0
	1.2	2.0
	4.8	1.0
10^2 c.p.s.	0.2	15.0
	1.0	6.7
	5.0	3.0
	20.0	1.5
10 c.p.s.	0.2	47.0
	1.0	21.0
	5.0	10.0
	20.0	5.0

This table shows the percent probable error for the count-rate meter at various counting rates and time constants.

one percent and to possess excellent long time stability. The circuit diagram is shown in Fig. (XV). The count rate meter has six ranges, from 1 c.p.s. to 10^5 c.p.s., with variable time constants for each range. Table I shows the percent probable error for the various time constants for each range.

In his report, Cooke-Yarborough gives a detailed analysis of the circuit, and outlines the procedure for "setting-up" the meter.

H. THE BROWN RECORDER

A Brown direct reading potentiometer Model No.153X12 is used to record the output of the count rate meter.

FIGURE XVI

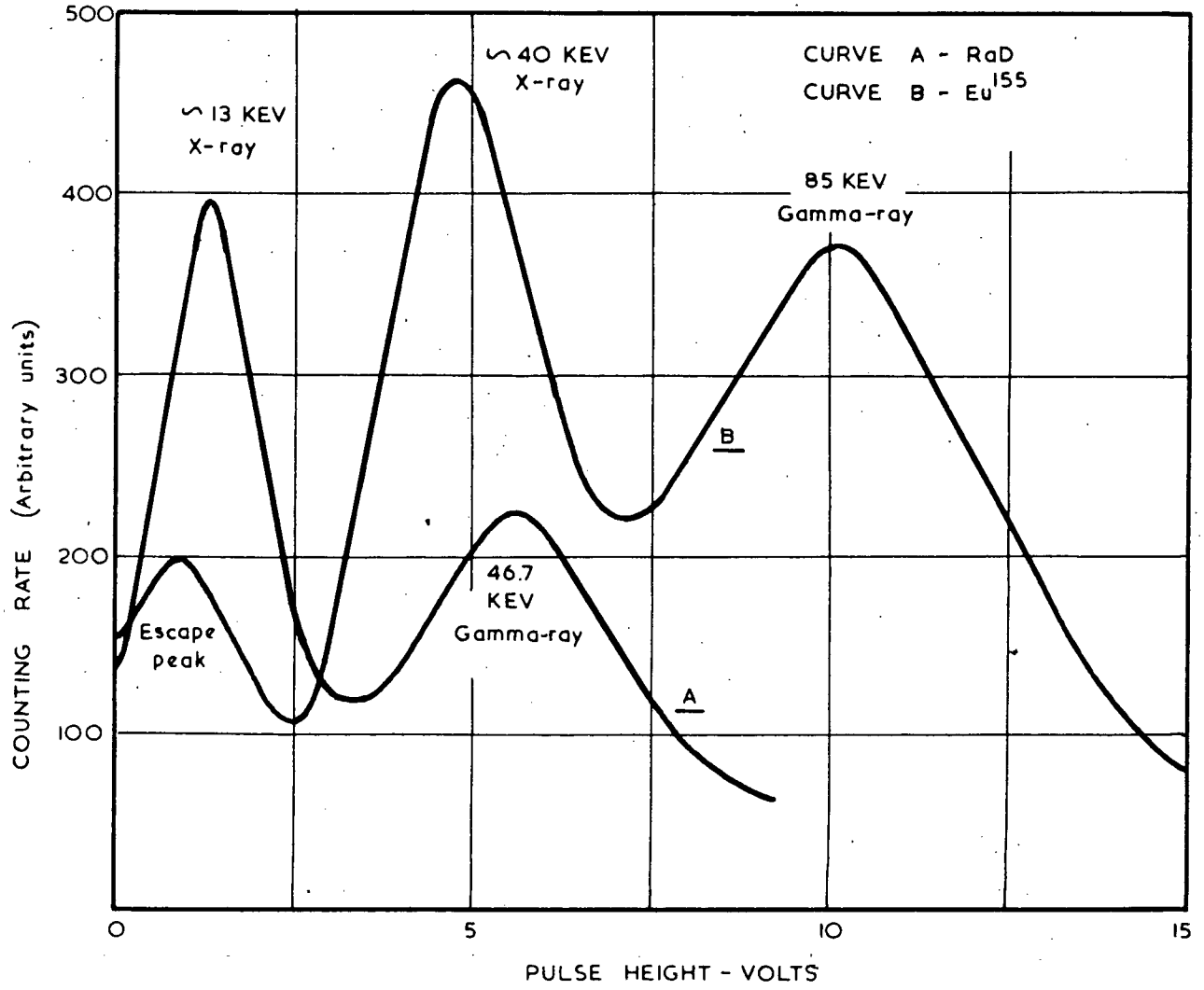

Pulse height distribution for RaD and Eu^{155} obtained with the thin cylindrical crystal.

V. EXPERIMENTAL RESULTS

The pulse height distributions for the gamma-rays of Eu^{155}, RaD, Na^{22}, Zn^{65} and RdTh have been obtained with different size crystals with a view to comparing the experimentally obtained shapes with the calculated shapes. These distributions have also been used to determine the conditions under which optimum resolution is obtainable with this technique and to calculate from the statistical formula for resolution (equation (2)), page 6) the effective number of photoelectrons produced at the photocathode per MeV of incident energy.

The distributions for each source are considered in detail below. The crystals with which the distributions were obtained are designated #1, #2, and #3 for the thin crystal (1/8" thickness, 1-3/4" diameter), the 3/4" x 3/4" x 1-1/2" block, and the 1/2" cube respectively.

A. RaD AND Eu^{155}

The distributions for these two sources are shown in Fig. (XVI) and were obtained with crystal #1. In the region below 20 KeV the resolution is very poor, approximately 100%, so that the precise determination of energy is impossible. From 20 KeV upward the resolution rapidly improves and is about 50% for the 85 KeV line in Europium. The crystal container was made as thin as possible (see Fig. (XI)) to increase the detection efficiency for low energy ($<$ 20 KeV) quanta. The mounting technique for this case was very difficult and usually resulted in a loss of efficiency of light collection and hence poorer resolution. More

work is being done to improve this technique, and by sacrificing some detection efficiency it should be possible to improve the resolution.

The relatively large 13 KeV peak in the RaD distribution shows the detection efficiency possible in this region. With better resolution it may be possible to resolve the escape peak which should appear at approximately 17 KeV. This would probably show as a change of slope or a "bump" on the high energy side of the 13 KeV peak.

The distribution for Eu^{155} shows the presence of the well known gamma-ray at 85 KeV and of a 40 KeV X-ray resulting from K- conversion de-excitation of the 85 KeV level in Gadolinium. The 100 KeV gamma-ray has not yet been resolved, but with the possible increase in resolution mentioned above and by manual operation of the Kicksorter baseline so that improved statistics are possible, the peak should appear. The distribution also shows the presence of a peak at 10 KeV which is presumably the escape peak due to photoelectric absorption of the 40 KeV X-ray. Mateosian and Smith (8) indicate a method of calculating the intensity of this peak. However, since no attempt has yet been made to measure absolute intensities, relative intensities, or conversion coefficients this calculation has not been carried through. If experiments of this type are to be done a correction for the wall effect in this thin crystal must be made.

An examination of Fig. (XVI) shows that there exists a small amount of non-linearity of response. If the RaD distribution is used as the calibration curve, it can be seen that the Eu^{155} dis-

tribution is shifted a small amount ($\approx$ 5%) in the low energy direction. The rapid deterioration of the MgO reflecting surface and hence the decrease in light collection efficiency is assumed to be responsible for this non-linearity, since considerable time elapsed between the runs on the two sources. As has been indicated above, further work is in progress to improve the technique in this energy region and it is fully expected that the non-linearity will be removed.

Mateosian and Smith (8) describe a method of obtaining spectra, both gamma and beta, by using a sodium iodide crystal which contains a small quantity of the source under investigation as an impurity. This method removes the difficulties introduced by the absorption of gamma-rays (or beta particle) in the crystal container, and in cases where source thickness is important, a source of effectively zero thickness is obtained. In experiments where this is not feasible it is possible to place the source in direct contact with the crystal, both source and crystal being enclosed by the container.

B. Na^{22}

The spectrum of Na^{22} consists of a 1.28 MeV gamma-ray and a 0.511 MeV annihilation radiation. Fig. (VII) shows the expected pulse height distribution for these two energies on the assumption that only primary processes occur. The ratios of the Compton peak height to the photopeak height are 0.92 and 3.6 for the 0.511 MeV and 1.28 MeV radiations respectively.

Figs. (XVII) and (XVIII) show the experimentally observed

FIGURE XVII

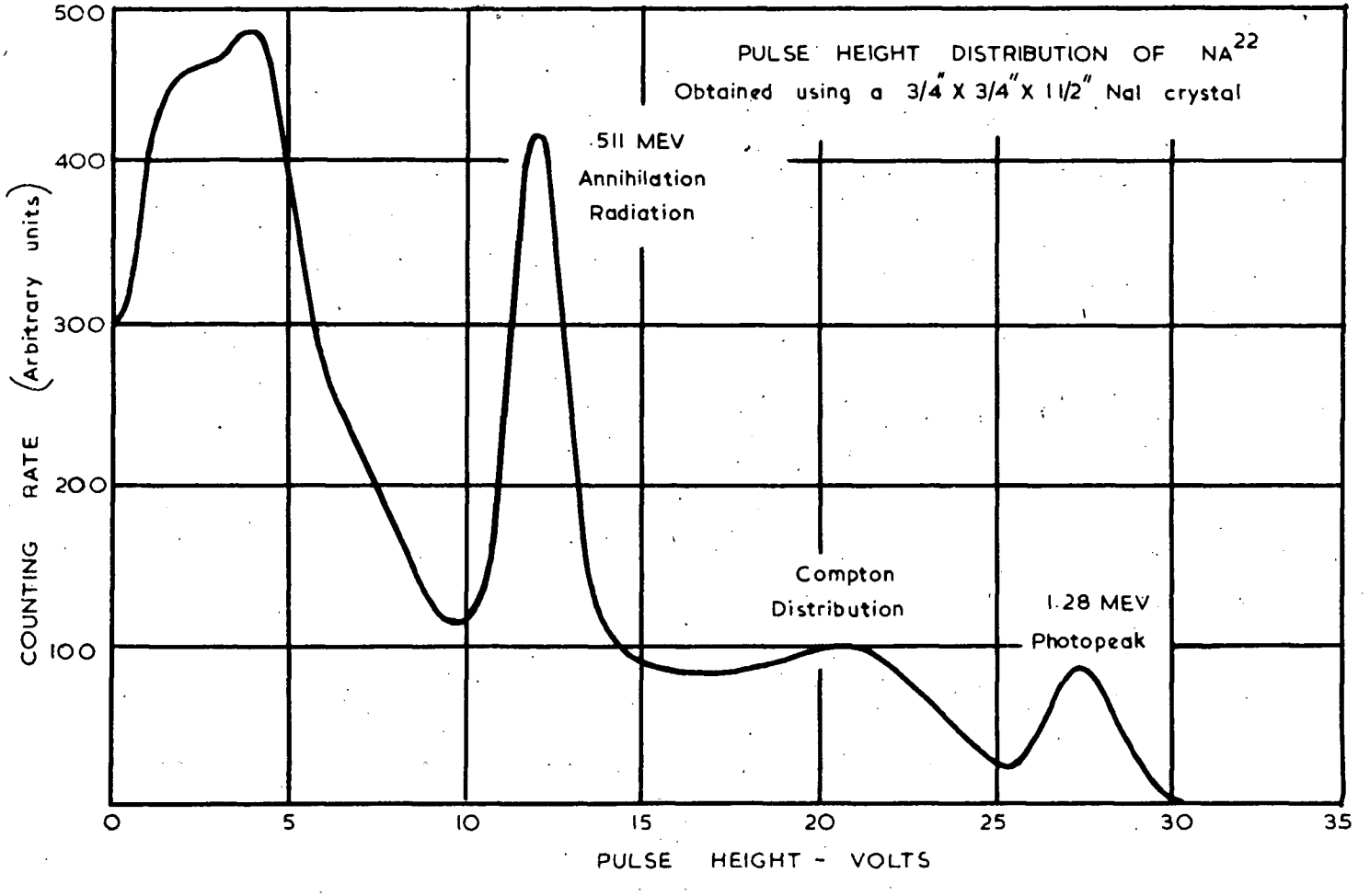
PULSE HEIGHT DISTRIBUTION OF NA22
Obtained using a 3/4" X 3/4" X 1 1/2" NaI crystal
511 MEV
Annihilation
Radiation
Compton
Distribution
1.28 MEV
Photopeak
COUNTING RATE (Arbitrary units)
500
400
300
200
100
0
5
10
15
20
25
30
35
PULSE HEIGHT - VOLTS

FIGURE XVIII

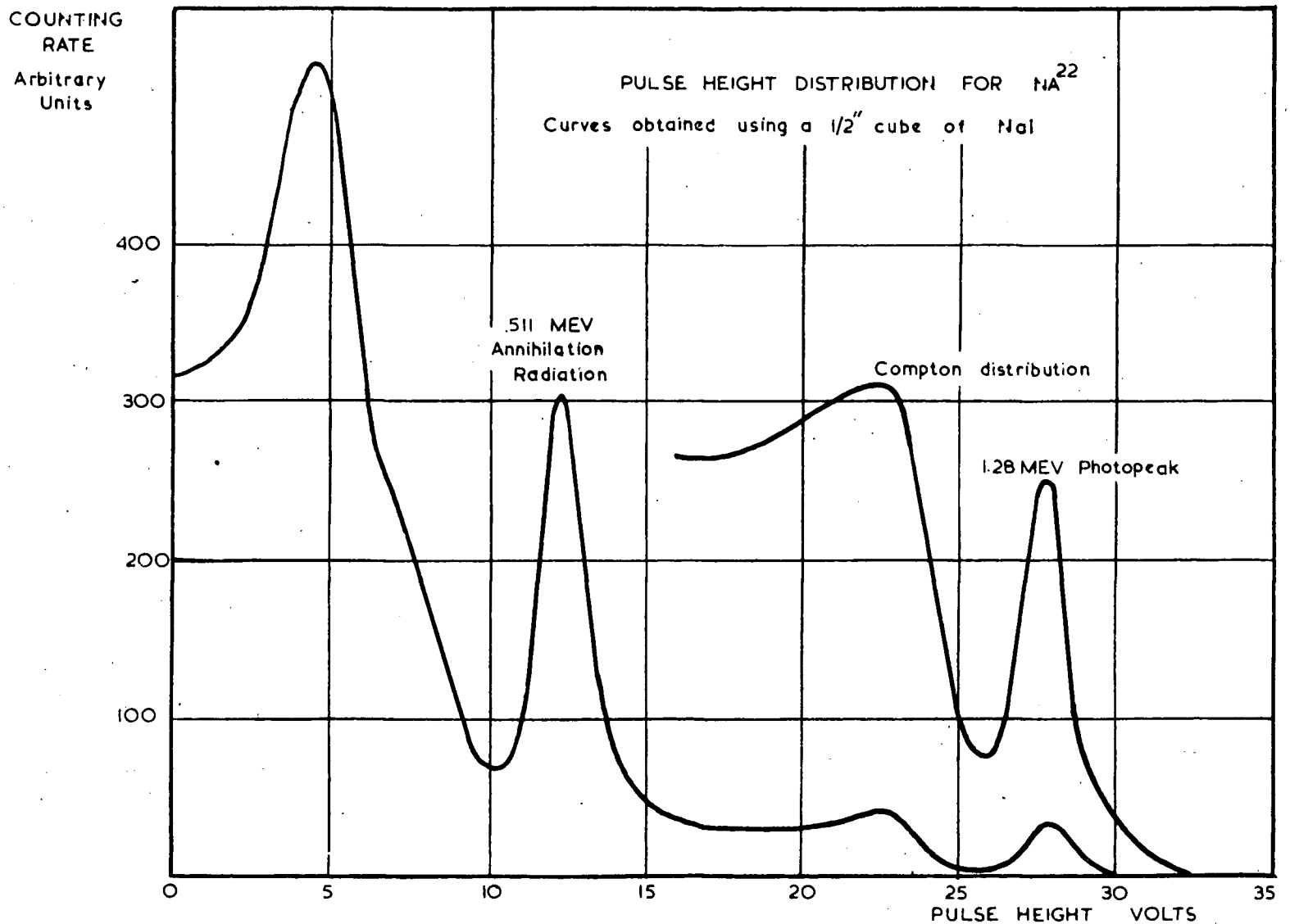

distribution obtained with crystals #2 and #3 respectively. Both of these curves have an intense low energy ($\approx$250 KeV) peak with the high energy side consisting of two components of different slope. It has been assumed that the point at which this change of slope occurs on each curve corresponds to the peak of the Compton distribution. The majority of the counts in these peaks, however, are assumed to be caused by back-scattered quanta ($\approx$ 250 KeV for 1 MeV radiation) originating in the walls of the crystal mounting, the photomultiplier tube, and surrounding objects. This second assumption can be supported by the following experimental evidence:

(i) A peak of approximately 250 KeV appeared in all the distributions whenever high energy ($>$ 500 KeV) gamma-rays were present.

(ii) Collimation of the incident beam reduced the intensity of the peak and changed its shape, but never eliminated it.

(iii) Without collimation the peak shape could be changed considerably (but not the relative intensity very much) by changing the position of the source. Under similar conditions the Compton and photoelectric distributions always remained constant in shape and relative intensity.

(iv) With similar source geometry, the peak took on different shapes for crystals of different dimensions but, again, the Compton and photoelectric distributions remained essentially the same

Aside from this rather intense low energy peak the shape of the distribution is roughly that expected from previous considerations. The relative intensities of the Compton and photopeaks

has been shown to be critically dependent on crystal dimensions as the result of multiple scattering events. This effect as a function of crystal dimensions is quite evident from the curves as can be seen if the ratio r = $\frac{\text{Compton peak height}}{\text{photopeak height}}$ for the 1.28 MeV radiation is considered. (The 0.511 MeV radiation is not considered since the Compton distribution is not well defined). The following values of r have been obtained:

(i) Calculated distribution (primary processes only) r = 3.6

(ii) Crystal #2 r = 1.1

(iii) Crystal #3 r = 1.25

The ratio increases as the dimensions become smaller thus verifying the qualitative arguments presented previously. The resolution also improves but this will be discussed separately in a following section.

The transferring of pulses from the Compton peak to the photoelectric peak by multiple scattering processes limits the accuracy of determining relative intensities by comparing areas under photopeaks. Although the 0.511 MeV Compton distribution is not well defined there is an indication that this effect is a function of energy as well as crystal dimensions. Consequently, a rigorous calculation must eventually be made on the magnitude of this process as a function of energy and crystal dimensions

C. Co^{60}

The Co^{60} spectrum is known to consist of two gamma-rays, 1.17 MeV and 1.33 MeV in cascade. The calculated distribution (primary processes only) is shown in Fig. (VIII) and the experi-

FIGURE XIX

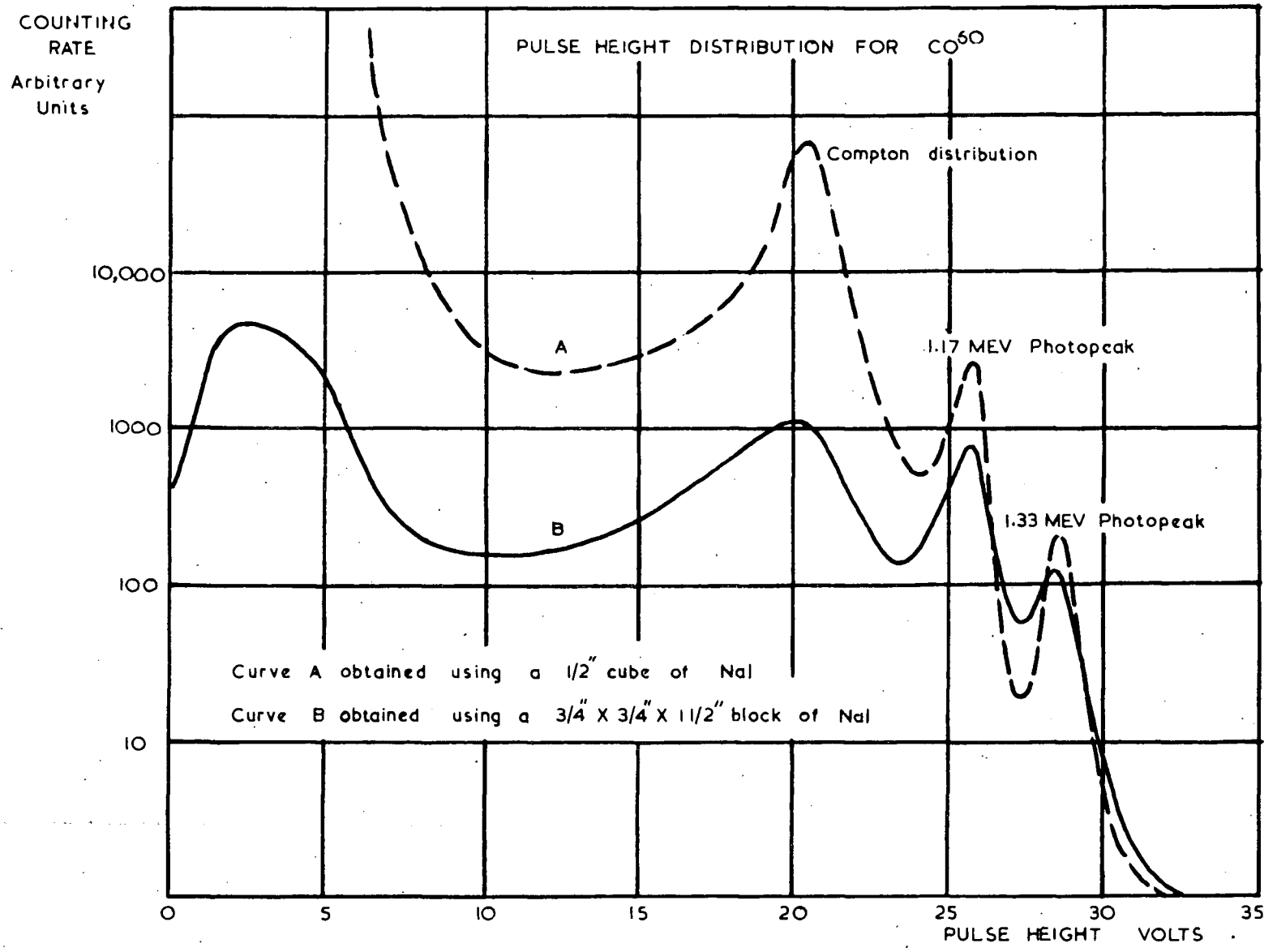
COUNTING RATE
Arbitrary Units
PULSE HEIGHT DISTRIBUTION FOR CO^{60}
Compton distribution
1.17 MEV Photopeak
1.33 MEV Photopeak
A
B
10,000
1000
100
10
Curve A obtained using a 1/2" cube of NaI
Curve B obtained using a 3/4" X 3/4" X 1 1/2" block of NaI
0
5
10
15
20
25
30
35
PULSE HEIGHT VOLTS

FIGURE XX

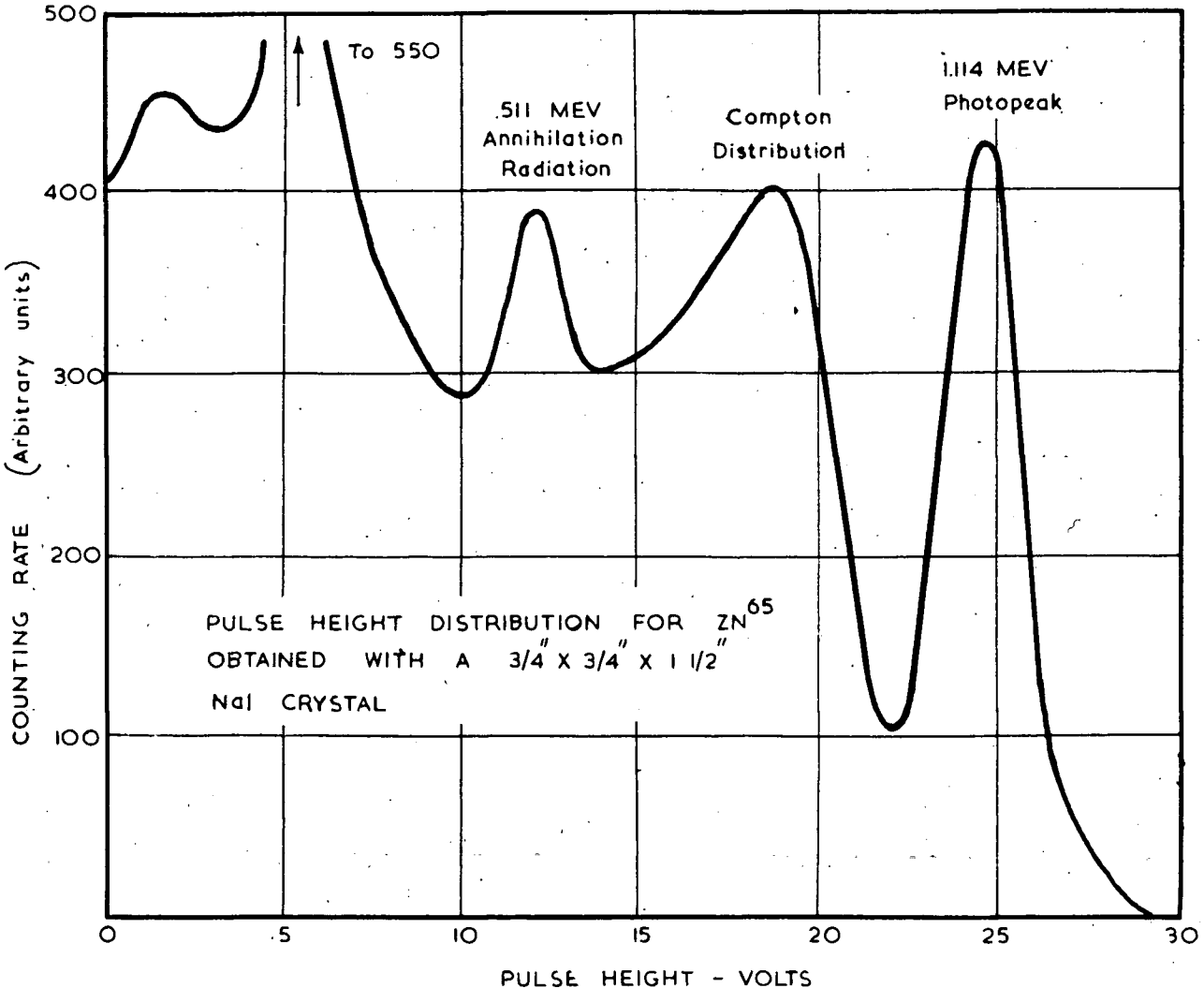
500
400
300
200
100
COUNTING RATE (Arbitrary units)
To 550
.511 MEV
Annihilation
Radiation
Compton
Distribution
1.114 MEV
Photopeak
PULSE HEIGHT DISTRIBUTION FOR ZN65
OBTAINED WITH A 3/4" X 3/4" X 1 1/2"
NaI CRYSTAL
0
5
10
15
20
25
30
PULSE HEIGHT - VOLTS

FIGURE XXI

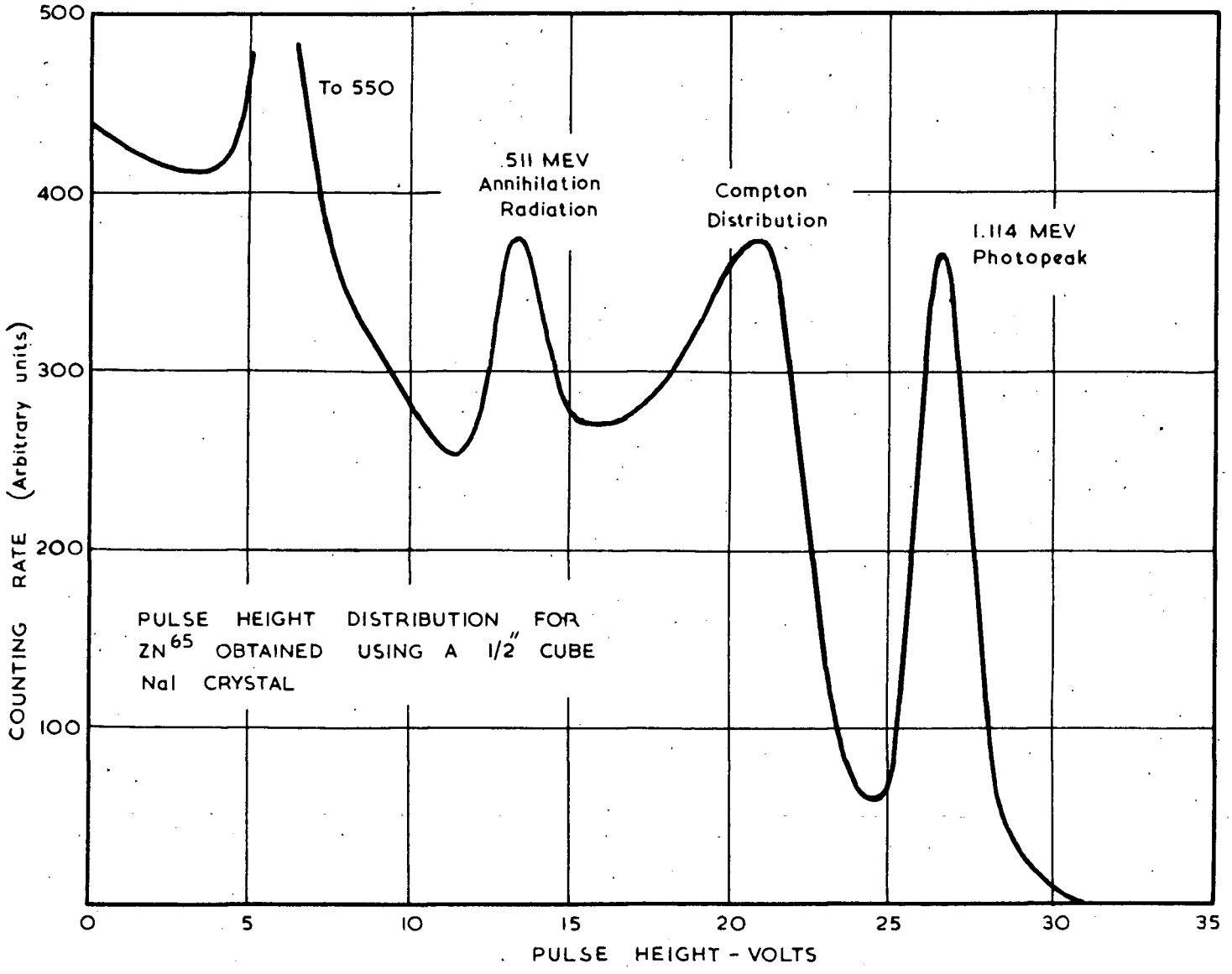
500
400
300
200
100
COUNTING RATE (Arbitrary units)
To 550
511 MEV
Annihilation
Radiation
Compton
Distribution
1.114 MEV
Photopeak
PULSE HEIGHT DISTRIBUTION FOR
ZN65 OBTAINED USING A 1/2" CUBE
NaI CRYSTAL
0
5
10
15
20
25
30
35
PULSE HEIGHT - VOLTS

mental distributions in Fig. (XIX). An intense low energy peak ($\approx$250 KeV) also appears in these distributions and is interpreted in a similar manner to that of Na^{22} in the previous section.

The effects of multiple scattering, again, are quite evident, and the values for the ratio r as defined in the preceeding section are:

(i) Calculated distribution

r(1.17 MeV) = 3.0 r(1.33 MeV) = 8.3

(ii) Crystal #2

r(1.17 MeV) = 1.05 r(1.33 MeV) = 1.45

(iii) Crystal #3

r(1.17 MeV) = 1.4 r(1.33 MeV) = 2.1

These ratios are larger for the smaller crystal, as expected, and the resolution is also markedly improved as will be described later. The importance of crystal dimensions is again emphasized by these curves, particularly by the increased height of the photopeaks due to the transfer of Compton pulses. The above ratios do not give a true picture since two Compton distributions are superimposed and the resolution was not sufficiently good to resolve them.

D. Zn^{65}

There are two main radiations in the gamma-ray spectrum of Zn^{65}: a 1.114 MeV line and 0.511 MeV annihilation radiation. The experimental distributions are shown in Fig. (XX) and (XXI) for crystals #2 and #3 respectively. Qualitatively, these distributions are very similar to those of Na^{22} except that the

FIGURE XXII

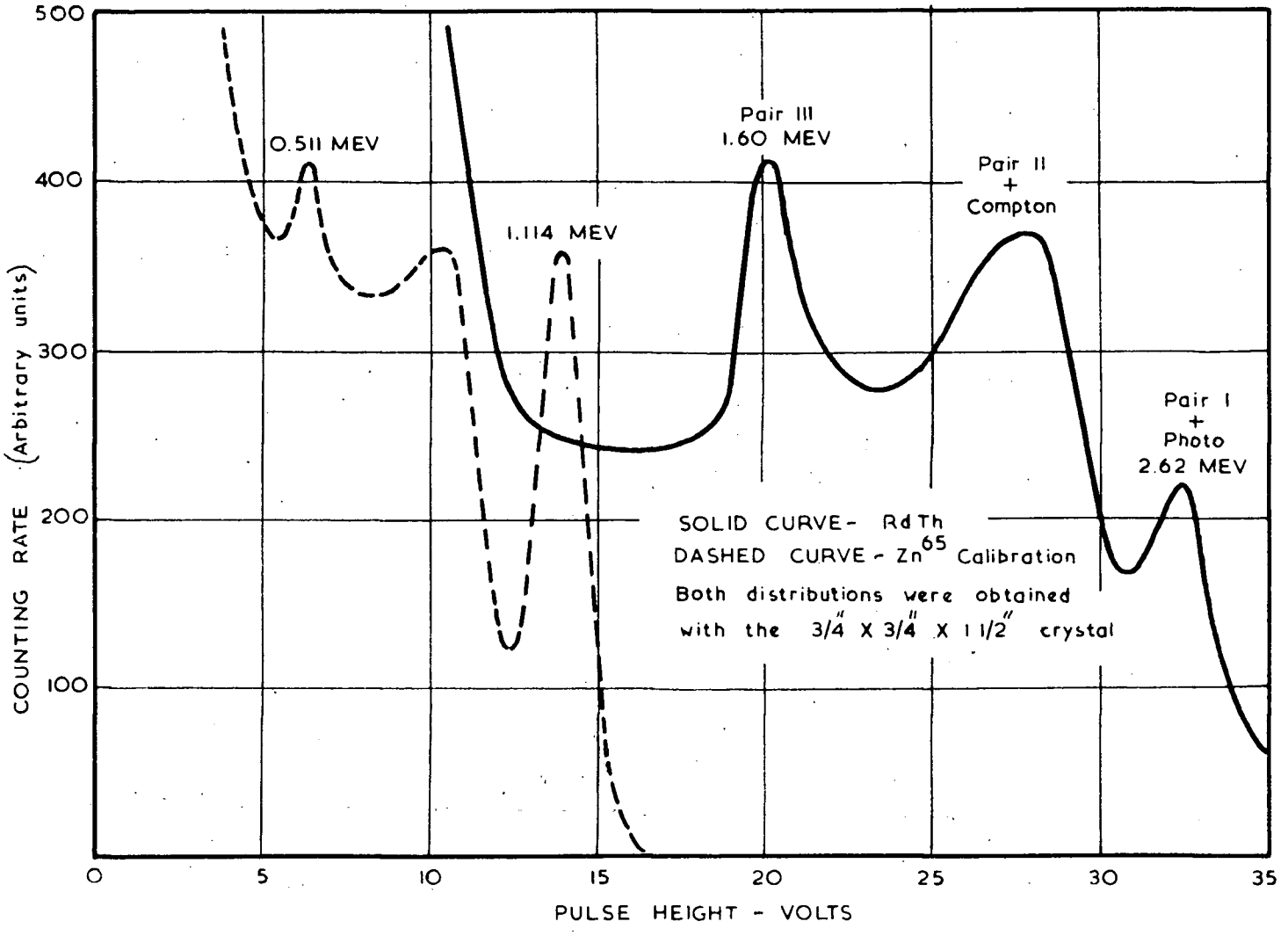
500
400
300
200
100
COUNTING RATE (Arbitrary units)
0.511 MEV
1.114 MEV
Pair III
1.60 MEV
Pair II
+
Compton
Pair I
+
Photo
2.62 MEV
SOLID CURVE- RdTh
DASHED CURVE - Zn65 Calibration
Both distributions were obtained
with the 3/4" X 3/4" X 1 1/2" crystal
0
5
10
15
20
25
30
35
PULSE HEIGHT - VOLTS

relative intensity of the annihilation radiation is much smaller

Hence an interpretation for these curves, similar to that for Na^{22} is valid. It will be noticed that the ratio r is not as different, (i.e. r = 0.94 and 1.02) as would be expected.

E. RdTh DISTRIBUTIONS

The radio-thorium spectrum has a number of gamma-ray lines less than 1 MeV in energy, and a reasonably strong one at 2.62 MeV. Since it was felt that the above results adequately covered the energy region below 1.5 MeV, the high energy end only of the radio-thorium spectrum was investigated.

At 2.62 MeV the pair production cross-section in NaI is significant so that the pair peaks should appear in this distribution. Fig. (XXII) shows the experimental distribution obtained with crystal #2. As was indicated on page 15 the relative intensities of the three pair peaks cannot be predicted on any reasonably simple theory so that no quantitative comparison with theory can be made. Qualitatively, however, these three peaks arise in the following manner:

(i) The low energy peak.

This peak is due entirely to the Pair III contribution and is superimposed on the low energy tail of the Compton distribution. Its position corresponds to 1.60 MeV.

(ii) The medium energy peak.

This peak is the sum of two contributions: the Compton distribution from the 1.28 MeV gamma-ray, and the Pair II distribution. The position of the peak cannot be predicted accura-

tely since the energy of the Compton peak is not known precisely, the Pair II distribution is broadened an indeterminate amount by multiple scattering of the absorbed annihilation quanta, and the relative contribution of each distribution is unknown

(iii) The high energy peak.

This peak consists of three components: the photoelectric contribution, the Pair I contribution, and the multiple scattering contribution from the Compton peak. Its position corresponds to 2.62 MeV and due to multiple scattering events the low energy side would be expected to be broadened.

The presence of these three well defined peaks in the distribution shows that when pair production occurs an accurate energy measurement is possible. The use of a larger crystal will increase the relative intensity of the high energy peak as well as increasing the efficiency of detection for high energy gamma-rays. If both the low and high energy peaks can be identified in an unknown distribution, an energy calibration is immediately possible since their difference in position corresponds to 1.02 MeV.

The appearance of three peaks in the pair production distribution has the disadvantage that if a spectrum consists of two or more gamma-rays differing in energy by 1.2 MeV or less, the resultant distribution will be very difficult to analyze, i.e., for two gamma-rays six peaks will be in a very small region. In many experiments where this occurs, the use of a single crystal scintillation counter is unsatisfactory and alternative schemes must be sought, e.g., the 3 crystal pair spectrometer (15).

F. ENERGY RESOLUTION

One of the main reasons for undertaking this work was to find the conditions under which optimum resolution is achieved for a given energy range. For the region below 100 KeV it was found that a thin crystal gives the best results, both in detection efficiency and in resolution. With additional work, further improvements are expected in this energy region.

In the energy range 0.5 MeV to 1.5 MeV it has been found that the small crystal gave the better resolution. Table II shows the resolution in % achieved with both crystals #2 and #3 for the peaks in the Na^{22}, Zn^{65}, and Co^{60} distributions. No values were assigned the 1.17 MeV photopeaks in the Co^{60} distributions since it was very difficult to determine their half heights. For the same reason, the resolution assigned to the 0.511 MeV peaks in Zn^{65} is subject to considerable error.

TABLE II

Crystal No.	Na^{22} .511 MeV Peak	Na^{22} 1.28 MeV Peak	Zn^{65} .511 MeV Peak	Zn^{65} 1.114 Mev Peak	Co^{60} 1.33 MeV Peak
#2	14.7	9.1	18.8	11.3	9.3
#3	12.7	8.0	12.2	8.0	7.0

The effective number of electrons produced at the photocathode per MeV of energy incident on the crystal has been calculated from the Na^{22} distributions using equation (2) page 21. The values obtained are 680 and 930 for crystals #2 and #3 respectively.

The values of A (see page 21) were found to be zero withing the accuracy of the calculations.

The smaller crystal gives better resolution as a result of the following two effects.

(i) Less broadening due to multiple scattering as has been previously emphasized.

(ii) Better light collection due to the smaller dimensions of the c rystal.

It should be noted the "n", the effective number of photocathode electrons per MeV is not a true values since the equation for calculating it does not include a factor accounting for broadening by multiple scattering.

It is concluded from these results that to about 2 MeV, the best resolution is achieved with a crystal of rather small dimensions ($< 1/2$" cube). A lower limit, of course, is set on the dimensions by:

1. The magnitude of the wall effect which increases with decreasing dimensions and higher energies, and

2. by the intensity of the radiation being measured in which case the dimensions must be chosen so that a reasonable counting rate is obtained.

It is doubtful whether further significant improvements in resolution will be obtained by additional work on mounting techniques. Improvements will have to wait on the development of more efficient phosphors and photocathode surfaces.

G. THE SEARCH FOR GAMMA-RAYS FROM TRITIUM

The triton is known to decay (14) to He^3 by beta-emission with an end point of approximately 18 KeV and with a half-life of approximately 12 years. A source of tritium* adsorbed in zirconium on a thick tungsten backing was investigated with the thin crystal to determine the presence, if any, of a low energy gamma-ray.

Since tritium decays by beta-emission, the pulse height distribution would consist mainly of a continuous distribution, cutting off at 18 KeV, as the result of brehmstrahlung radiation from the beta-particles. Any low energy peak would be superimposed on this continuous distribution. With the resolution achieved with the thin crystal, it would be necessary for a gamma-ray to be greater than 7 KeV in energy and at least comparable (to an order of magnitude) in intensity to the brehmstrahlung radiation, to be detectable. To this degree of experimental accuracy, there is no indication of the presence of a gamma-ray.

The distribution had a plateau at a very low energy, partly obscured by the large noise background. It was thought at first that this plateau resulted from the presence of a gamma-ray. However, by inserting thin aluminum absorbers (from .001" to .015") between the source and the counter it was found that the plateau developed into a peak, and as the absorber thickness was increased the peak shifted upward in energy to a maximum of 18 KeV. The intensity, of course, dropped rather drastically. Since

* Obtained from the Atomic Energy Commission of Canada.

the absorption of gamma-rays increases very rapidly with a decrease in energy the above phenomena was attributed to the increasing absorption of the lower energy quanta in the continuous brehmstrahlung distribution. The fact that the upward shift in peak energy ceased at 18 KeV verifies this. A similar experiment was done with the 13 KeV peak in the RaD distribution. No shift in the energy of the peak was noticed with increasing absorber thickness. From this, and the above argument it was concluded that the plateau in the tritium distribution was not due to a low energy gamma-ray.

APPENDIX I

Calculation of the Compton Electron Distribution.

The formula obtained on page 9 for the Compton electron distribution is

$$\frac{d_e\sigma}{dE_{el}} = \frac{2\pi}{\alpha h\nu} k(\theta)\left\{\frac{(1+\alpha)^2 - \alpha^2\cos^2\phi}{(1+\alpha)^2 - \alpha(2+\alpha)\cos^2\phi}\right\}^2 \qquad (1)$$

where $k(\theta)$ is given by eqn. (6) page 7

This equation can be simplified giving equation (16) page 10 by converting the units of the electron energy to $\alpha_{el} = \frac{E_{el}}{mc^2}$

(a) The simplification of $\cos^2\phi$

$$E_{el} = h\nu\left\{\frac{2\alpha}{(1+2\alpha) + (1+\alpha)^2\tan^2\phi}\right\} \qquad \text{see eqn. (3) page 6}$$

Solving this equation for $\cos^2\phi$, the result is

$$\cos^2\phi = \frac{\alpha_{el}}{\alpha}\ \frac{(1+\alpha)^2}{2+\alpha_{el}} \qquad (2)$$

(b) A similar simplification for cos θ gives

$$\cos\theta = 1 - \frac{\alpha_{el}}{\alpha(\alpha-\alpha_{el})} \qquad (3)$$

(c) The expression for $k(\theta)$ given on page 6 can be simplified with the use of equation (3) above and the new energy units, giving

$$k(\theta) = \frac{r_o^2}{2\alpha^2}\left\{\frac{1}{\alpha^2}\left[2\alpha^2(\alpha-\alpha_{el})^2 - 2\alpha\alpha_{el}(\alpha-\alpha_{el}) + \alpha_{el}^2 + \alpha\alpha_{el}^2(\alpha-\alpha_{el})\right]\right\} \qquad (4)$$

Then using equations (2) and (4), equation (1) becomes

$$\frac{d_e\sigma}{dE_{el}} = \frac{\pi r_o^2}{\alpha^2 mc^2}\left\{2 + (\alpha_{el}-2)\left[\frac{\alpha_{el}}{\alpha(\alpha-\alpha_{el})}\right] + \left[\frac{\alpha_{el}}{\alpha(\alpha-\alpha_{el})}\right]^2\right\}$$

APPENDIX II

THE SCINTILLATION OF ALPHA PARTICLES IN AIR

As a preliminary to the investigation of the scintillations produced by ionizing particles in gasses and vapours, the scintillations produced in air by alpha particles have been examined. This investigation was carried out in the following manner:

(i) A polonium alpha source was mounted in a light tight box.

(ii) The interior of the box was viewed with an R.C.A. 5819 photomultiplier so situated that any scintillations produced by the alpha particles would be detected.

(iii) The source was so placed that its self-luminescence could not reach the photomultiplier. A suitable shutter was constructed such that the alpha particles could, when desired, be prevented from traversing the box.

(iv) The counting rate from the photomultiplier was measured with the shutter "covering" the source and with the shutter removed from the alpha particle beam.

A significant increase, approximately eight times the background, was observed when the alpha particles were allowed to traverse the box. This increase was attributed to the scintillations produced in the air within the box. The pulse amplitudes were small, of the same order as large noise pulses, but the light collection was not very efficient.

This preliminary investigation established the existence of the effect. In view of the meagre information on the number of photons and their energy produced by ionizing events in gasses,

further work is indicated; namely the variation of the effect with pressure and with the nature of the gas. The theoretical side of this problem, unlike the associated one where ion pairs are produced, has been little discussed. However, the publication by Grun and Schopper (16) showed that this line of work was more advanced elsewhere, and since the author's main interest was in the investigation of gamma-ray spectra with scintillation counters, the above work was discontinued.

This effect could clearly be responsible for some of the strange results reported by Richards and Cole (17) and Richards and Dee (18).

BIBLIOGRAPHY

(1)	Hofstadter	Physical Review	74, 100, 1948
(2)	Hofstadter and McIntyre	Physical Review	78, 617, 1950
(3)	Hofstadter and McIntyre	Physical Review	79, 389, 1950
(4)	Hofstadter	Physical Review	80, 631, 1950
(5)	Swank and Moenich	Rev.Sci. Instruments	23, 502, 1952
(6)	Klein and Nishina	Z.Physik	52, 853, 1929
(7)	Davisson and Evans	Review of Modern Physics	24, 79, 1952
(8)	der Mateosian and Smith	Physical Review	88, 1186, 1952
(9)	Roberts	Proc.Physical Society A,	192, 1953
(10)	Gillette	Report for the Linde Air Products Co. Tonawanda, New York.	
(11)	Westcott and Hanna	Rev.Sci.Instruments	20, 181, 1949
(12)	Elmore and Sands	Electronics	McGraw Hill, 1949
(13)	Cooke-Yarborough	Proc.Inst.Elect.Engs. Part II	98, 191, 1951
(14)	Langer and Moffat	Physical Review	88, 689, 1952
(15)	Johansson	Phil. Magazine	43, 249, 1952
(16)	Grun and Schopper	Z.Naturforsch.	6A, 698, 1951
(17)	Richards and Cole	Nature	167, 286, 1951
(18)	Richards and Cole	Nature	169, 736, 1951